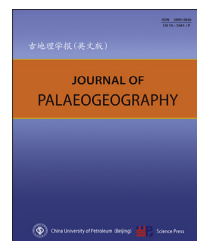




Available online at www.sciencedirect.com

ScienceDirect

journal homepage: <http://www.journals.elsevier.com/journal-of-palaeogeography/>



Tectonopalaeogeography and palaeotectonics

Petrography and tectonic provenance of the Permian Tunas Formation: Implications on the paleotectonic setting during the Claromecó Foreland Basin evolution, southwestern Gondwana margin, Argentina



Maria Belén Febbo^{a,b,c,}, Renata N. Tomezzoli^{a,d},
Nora N. Cesaretti^{b,c}, Giselle Choque^{b,c},
Natalia B. Fortunatti^{b,c}, Guadalupe Arzadún^{a,e}*

^a Consejo Nacional de Investigaciones Científicas y Técnicas (CONICET), Argentina

^b Dpto. de Geología, Universidad Nacional del Sur, Avenida Alem 1253, B8000ICP, Bahía Blanca, Argentina

^c Centro de Geología Aplicada y Medio Ambiente (CGAMA, CIC-UNS), Dpto. de Geología, Universidad Nacional del Sur, Bahía Blanca, Argentina

^d Laboratorio de Paleomagnetismo "Daniel A. Valencio", Instituto de Geociencias Básicas, Aplicadas y Ambientales de Buenos Aires (IGEBA), Departamento de Ciencias Geológicas, Facultad de Ciencias Exactas y Naturales (FCEyN), Universidad de Buenos Aires (UBA), Pabellón II (1428), CABA, Argentina

^e Laboratorio de Termocronología (La.Te Andes-CONICET), Las Moreras 310, A4401XBA, Vaqueritos, Salta, Argentina

Abstract The Claromecó Basin is located at the south-western sector of the Buenos Aires province, Argentina. This basin is considered a foreland basin closely related to the evolution of the southwestern Gondwana margin. This contribution focuses on the provenance analysis of the Tunas Formation (Permian, Pillahuincó Group), which represents the last filling stage for the Claromecó Foreland Basin. Petrographic and tectonic provenance analyses were performed in sandstones recovered from subsurface (PANG 0001 and PANG 0003 exploration wells) and outcrops located close to the basin center (Gonzales Chaves locality). In the subsurface, the analyzed succession is composed of medium- to fine-grained sandstones interbedded with tuffs, mudrocks, carbonaceous mudrocks and coal beds. In outcrops, the succession is dominated by medium- to fine-grained sandstones interbedded with siltstones. Modal composition patterns are distributed into the recycled orogen and transitionally recycled to mixed fields. Petrographic analyses, in addition to provenance and sedimentological studies, confirm that sedimentary material was derived from a mixed source, which largely comes from the Sierras Australes fold and thrust belt, located towards the W-SW, where the sedimentary succession is interbedded with volcanic material. The Tunas Formation shows clear differences in its modal composition, paleocurrent direction and paleoenvironmental conditions with respect to the underlying

* Corresponding author. Dpto. de Geología, Universidad Nacional del Sur, Avenida Alem 1253, B8000ICP, Bahía Blanca, Argentina.
E-mail address: belenfebbo@gmail.com (M.B. Febbo).

Peer review under responsibility of China University of Petroleum (Beijing).

<https://doi.org/10.1016/j.jop.2022.06.001>

2095-3836/© 2022 The Author(s). Published by Elsevier B.V. on behalf of China University of Petroleum (Beijing). This is an open access article under the CC BY-NC-ND license (<http://creativecommons.org/licenses/by-nc-nd/4.0/>).

units of the Pillahuincó Group (Sauce Grande, Piedra Azul and Bonete formations). Source areas changed from cratonic to mixed fold belt/arc-derived material, suggesting variations in the Claromecó Basin configuration during the Late Paleozoic. Changes in the paleotectonic scenario during the deposition of the Tunas Formation have been interpreted as a consequence of a compressive post-collisional deformation event, the product of adjustment, accommodation and translation of terrains towards the equator during the Permian–Triassic to form Pangea.

Keywords Provenance area, Petrography, Tunas Formation, Claromecó Foreland Basin, Southwestern Gondwana margin, Permian, Upper Paleozoic

© 2022 The Author(s). Published by Elsevier B.V. on behalf of China University of Petroleum (Beijing). This is an open access article under the CC BY-NC-ND license (<http://creativecommons.org/licenses/by-nc-nd/4.0/>).

Received 29 November 2021; revised 29 April 2022; accepted 29 April 2022; available online 9 June 2022

1. Introduction

Provenance studies in sedimentary rocks of foreland basins have been used to determine the paleogeography and tectonic evolution of adjacent orogenic belts (Dickinson and Suczek, 1979; Dickinson et al., 1983; DeCelles, 1986; DeCelles and Hertel, 1989). The sandstone modal composition is a useful tool to define the source areas and paleotectonic settings throughout basin evolution (Dickinson, 1970; Dickinson and Suczek, 1979; Dickinson et al., 1983; Zuffa et al., 1995). The composition of detrital constituents from sedimentary rocks depends on provenance area, but also is influenced by paleoclimate, weathering, transport agents and mechanisms, distance from source area, depositional environment and diagenesis (Dickinson and Suczek, 1979; McBride, 1985; DeCelles and Hertel, 1989, among others).

The Claromecó Basin is located in southern Buenos Aires province (~37°–39°S Latitude, 61°–63°W Longitude, Fig. 1A), Argentina. This basin was a part of the southwestern margin of the Gondwana supercontinent during the Late Paleozoic (Keidel, 1916, 1921; Du Toit, 1927; Harrington, 1947). This basin extends from the Sierras Australes fold and thrust belt (also known as Sierras de la Ventana o Ventana System) to the northeast, underlying Cenozoic deposits, and towards the Argentinian continental platform, covering a total area of 65,000 km². Pángaro et al. (2015) expanded its limits encompassing the Chaco-Paraná Basin (South America) and the Kalahari-Karoo Basin (South Africa), redefining it as the Hesperides Basin. Geophysical data and exploration wells revealed the existence of coal-bearing deposits corresponding to the Piedra Azul and Tunas formations (Lesta and Sylwan, 2005; Arzadún et al., 2016a, 2017; Febbo et al., 2017, 2018a; Zavala et al., 2019). Coal layers recorded in subsurface

can reach thickness of 0.5 m–4.5 m (Arzadún et al., 2016a, 2017; Febbo et al., 2017, 2018a, 2021, 2022; Zavala et al., 2019).

The Claromecó Basin has been interpreted as a foreland basin developed during the Carboniferous–Permian (Ramos, 1984; López-Gamundí and Rossello, 1992; Ramos and Kostadinoff, 2005; Tomezzoli, 2012) in response to flexural loading, due to the deformation and uplift of the Sierras Australes. The basin tectonic evolution is related to the accretion of terranes and microplates to the Gondwana's southwestern margin during the Middle Paleozoic or even the Triassic (Ramos, 1984, 2008; Tomezzoli and Vilas, 1997, 1999; Tomezzoli, 2001, 2012; Ramos and Kostadinoff, 2005; López-Gamundí, 2006; Pángaro and Ramos, 2012; Ramos and Naipauer, 2014). However, the geologic evolution and deformation of the Sierras Australes and the adjacent Claromecó Basin are still under debate.

The Tunas Formation (Early Permian; Harrington, 1947; López-Gamundí et al., 2013; Arzadún et al., 2018) is the youngest unit of the Pillahuincó Group, representing the last stage of the Paleozoic basin filling. The synorogenic Tunas Formation deposits have been considered of great relevance to understanding the Sierras Australes and Claromecó Basin evolution, and represent potential economic resources due to the presence of coal-bearing layers and associated gas (Arzadún et al., 2016a, 2017; Febbo et al., 2017, 2018a, 2022; López-Gamundí and Rossello, 2021). This unit clearly records changes in depositional conditions and paleogeographic and paleotectonic scenarios along the southwestern Gondwana margin during the Late Paleozoic. These changes confirmed the difference in sandstone modal compositions, the reversal of paleocurrent directions and the contemporary volcanic eruptive activity that could be recognized in the geological record (Andreis and Cladera, 1992; López-

Gamundi *et al.*, 1995; López-Gamundi and Rosello, 1998). Provenance studies for the Tunas Formation outcrops from the Sierras Australes fold and thrust belt area were performed by several authors (e.g., Andreis and Cladera, 1992; López-Gamundi *et al.*, 1995; López-Gamundi and Rosello, 1998; Alessandretti *et al.*, 2013; Ramos *et al.*, 2014; Ballivián Justiniano *et al.*, 2020). However, this is the first work in which

the subsurface record of the Claromecó Basin was studied.

This contribution presents petrographic and tectonic provenance studies for the Tunas Formation from the subsurface (PANG 0001 and PANG 0003 exploration wells; Fig. 1) and outcrop data (the Gonzales Chaves locality; Fig. 1) of the Claromecó Foreland Basin area. The obtained data are integrated with previous

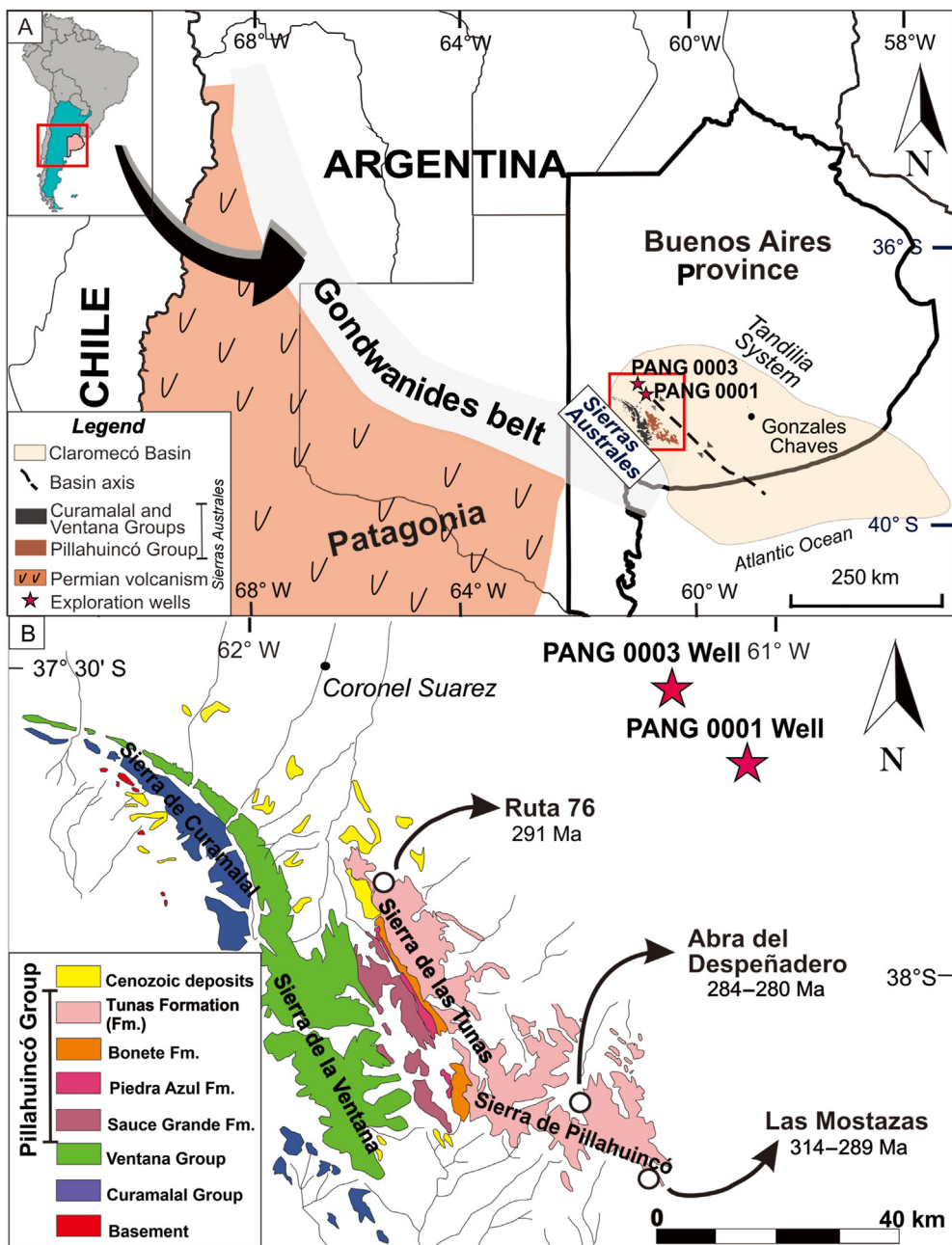


Fig. 1 A) Location map of the Claromecó Basin, PANG 0001 and PANG 0003 exploration wells and the Gonzales Chaves locality. Basin limits were defined by Kostadinoff and Font de Affolter (1982); B) Geological map of the Sierras Australes (modified from Suero, 1972) showing Tunas Formation outcrops, locations of PANG 0001 and PANG 0003 wells, and localities of U–Pb dating obtained by Arzadún *et al.*, (2018; Ruta 76), Tohver *et al.*, (2008; Abra del Despeñadero), Alessandretti *et al.*, (2013; Abra del Despeñadero), López-Gamundi *et al.*, (2013; Abra del Despeñadero), and Ballivián Justiniano *et al.*, (2020; Las Mostazas).

published results to better understand the paleogeographic and paleotectonic context during the deposition of the Tunas Formation and the evolution of the Claromecó Basin in the southwestern Gondwana margin during the Late Paleozoic.

2. Geologic and stratigraphic setting

The study area is located in the northwestern area of the Claromecó Basin in southern Buenos Aires province, Argentina (Fig. 1A). The origin of the Claromecó Basin was defined based on gravimetric studies, which revealed a sedimentary infill with a maximum thickness of 9 km–10.5 km (Kostadinoff and Font de Affolter, 1982; Introcaso, 1982). Its main axis is oriented NW–SE, parallel to the Tandilia System and the Sierras Australes trend (Kostadinoff and Font de Affolter, 1982; Ramos and Kostadinoff, 2005; Álvarez, 2007, Fig. 1A). The Paleozoic sedimentary infill of the Claromecó Basin is exposed along the Sierras Australes and underlies the Cenozoic sedimentary cover to the east–northeast, limiting with the Tandilia System, with some isolated outcrops near Gonzales Chaves locality (Fig. 1A). Seismic data and offshore exploration wells confirm the basin extension toward the Argentinian continental platform (Lesta et al., 1978; Lesta and Sylwan, 2005; Pángaro and Ramos, 2012), constituting the pre-rift basement of the Colorado Basin (Fryklund et al., 1996).

The tectonic evolution of the Sierras Australes and the adjacent Claromecó Basin is complex and recorded multiple compressional and extensional tectonic events throughout the Paleozoic–Mesozoic (Arzadún et al., 2020). Ramos and Kostadinoff (2005) proposed that the basin developed in three stages, from the Early to the Late Paleozoic: a rifting phase during the Early Paleozoic followed by a passive margin period from the Ordovician to the Devonian, and finally, the development stage of a foreland basin from the Carboniferous up to the Early Permian. Some authors interpreted the establishment of an active margin as resulting from the Patagonia terrane collision with the southwestern Gondwana margin during the Late Paleozoic (Ramos, 1984, 2008; Lesta and Sylwan, 2005; Pángaro and Ramos, 2012; Ramos and Naipauer, 2014). However, other authors considered that collision events began in the Chánica Orogenic phase during the Middle Devonian (Azcuy and Caminos, 1987) and continued up to the Permian (Tomezzoli, 1999, 2001, 2012; Arzadún et al., 2021). The compressive regime ended at the Late Paleozoic–Early Mesozoic boundary as the continents moved towards the equator to finally

configure Pangea during the Triassic (Tomezzoli, 2009; Gallo et al., 2017). During the Mesozoic, several rifting events affected the southern part of this area due to the formation of the Colorado Basin on the Argentinian continental platform (Lovecchio et al., 2018, 2020; Arzadún et al., 2020).

Deformation and uplift of the Sierras Australes were related to the Gondwanides Orogeny of Late Paleozoic age (Keidel, 1916; Du Toit, 1927; Milani and De Wit, 2008). Ramos (1984, 2008) proposed that the deformation of the Sierras Australes was linked to the accretion of the Patagonia terrane between Carboniferous and even late Early Triassic (Pángaro and Ramos, 2012). In contrast to the collisional model, other authors suggested an intracontinental deformation resulting from continental blocks which moved producing crustal fragmentation through strike-slip faults (Japas, 1989; Cobbold et al., 1991; Kostadinoff, 1993, 2007; Álvarez, 2004; Gregori et al., 2008; Vizán et al., 2015). According to Tomezzoli (2001, 2012), the deformation might have been a combination of these mentioned processes, with a collisional phase occurring during the Devonian–Carboniferous and a later post-collisional spasmodic deformation (Arzadún et al., 2021). These deformation events were associated with latitudinal movements due to the adjustment and coupling of terrains during the Permian–Triassic, to form Pangea, with a climax of the deformation during the Early Permian (~290 Ma) (Tomezzoli, 2012; Arzadún et al., 2021).

The Paleozoic sequence outcropped at the Sierras Australes displays a decreasing deformation from west to east (Harrington, 1947; von Gosen et al., 1991; Tomezzoli, 1999). The Lower Paleozoic successions (Curamalal and Ventana Groups; Fig. 1B) display a lower greenschist metamorphism (Cobbold et al., 1986; Buggisch, 1987), while the Upper Paleozoic sequences (Pillahuincó Group; Figs. 1B and 2A) present a very low-grade metamorphism to high diagenesis (Buggisch, 1987; von Gosen et al., 1991). Anisotropy of magnetic susceptibility (AMS) studies of the Tunas Formation from the Sierras Australes area (Tomezzoli, 2001; Arzadún et al., 2016b, 2021) and in the Claromecó Basin subsurface (Febbo et al., 2021) confirm a decrease in the magnitude of deformation towards the foreland basin during the Permian.

The Curamalal Group (Late Cambrian–Ordovician; Fig. 1B; Harrington, 1947) is a 1200 m-thick succession deposited in a stable marine platform, starting with a basal conglomerate (La Lola Formation), and it is mostly composed of quartzite with mudrock intercalations toward the top (Mascota, Trocadero and Hinojo Formations). The Ventana Group (Silurian–Middle

Devonian; Fig. 1B; Harrington, 1947) is a 1200–1400 m-thick succession deposited under stable marine conditions. This unit consists of sandstones with conglomerate lenses (Bravard Formation), quartzites (Napostá Formation), quartzites interbedded with sandstones and mudrocks (Providencia Formation), and mica-rich sandstones with slates and schist layers (Lolén Formation) (Harrington, 1947, 1972).

The Upper Paleozoic succession of the Claromecó Basin comprises the Pillahuincó Group, which is subdivided into four formations: Sauce Grande Formation, Piedra Azul Formation, Bonete Formation and Tunas Formation (Fig. 2A; Harrington, 1947). These units outcropped in the eastern portion of the Sierras Australes (Fig. 1) and reach a maximum thickness of approximately 2800 m (Harrington, 1970; López-Gamundí et al., 1995). The Pillahuincó Group is composed of glaciomarine deposits of the Sauce Grande Formation (Harrington, 1970), equivalent to the Dwyka Group in the Karoo Basin (López-Gamundí and Rossello, 1998), of a Late Carboniferous age (Pennsylvanian–Cisuralian; di Pasquo et al., 2008). This unit

consists of diamictites, sandstones and mudrocks and has a maximum thickness of 1100 m (Andreis et al., 1987). Glacial conditions ceased during the Early Permian (Gallo et al., 2020, and references therein), when shallow marine mudstones and sandstones, corresponding to the Piedra Azul and Bonete formations, progressively replaced diamictite deposits (Harrington, 1947). The presence of *Eurydesma* fauna and *Glossopteris* flora indicates an Early Permian age for these units (Archangelsky and Cúneo, 1984, Fig. 2A).

The Tunas Formation was deposited in deltaic to fluvial environments, representing the regressive culmination characterized with shallow marine conditions (Andreis et al., 1989; López-Gamundí et al., 1995, 2013; Andreis and Japas, 1996; Zorzano et al., 2011; Arzadún et al., 2017; Zavala et al., 2019; Ballivián Justiniano et al., 2020). This unit is exposed north of Sierras de las Tunas and south of Sierra de Pillahuincó (Fig. 1B), with small isolated outcrops near Gonzales Chaves locality ($S38^{\circ}03'18''$, $W60^{\circ}03'57''$; Fig. 1A) (Monteverde, 1937; Furque, 1965; Harrington, 1970; Llambías and Prozzi, 1975; Tomezzoli and Vilas, 1997;

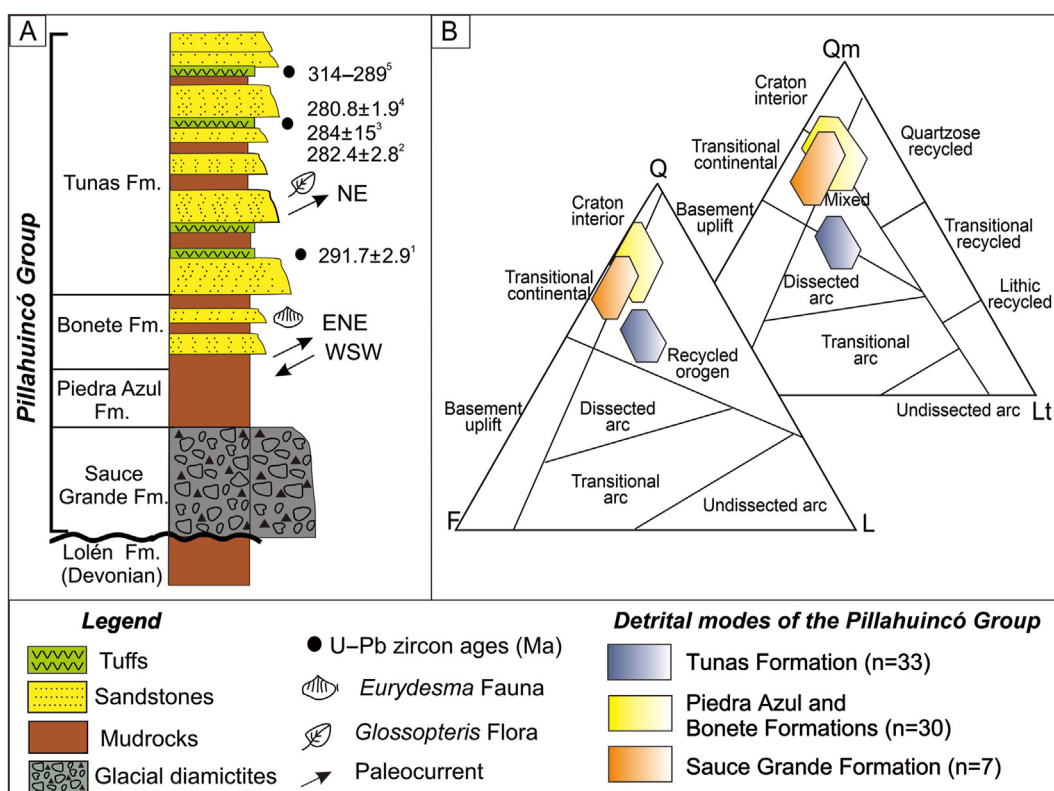


Fig. 2 A) Stratigraphic column of the Upper Paleozoic Pillahuincó Group (based on Harrington, 1947; Suero, 1972). Paleocurrents from Andreis and Japas (1991) and López-Gamundí et al. (1994). U–Pb zircon ages from tuff levels of Tunas Formation reported by Arzadún et al. (2018)¹, Tohver et al. (2008)², Alessandretti et al. (2013)³, López-Gamundí et al. (2013)⁴ and Ballivián Justiniano et al. (2020)⁵, located at different levels of the sequence; B) Detrital modes of the Pillahuincó Group plotted in the Dickinson et al. (1983) provenance diagrams, modified from López-Gamundí et al. (1995). Notice differences in the provenance areas among the lower units (Sauce Grande, Piedra Azul and Bonete formations), with a cratonic source and the Tunas Formation, with recycled orogeny/mixed-dissected arc source.

(Febbo et al., 2018b). Sedimentary deposits are composed of fine- to medium-grained greenish and yellowish sandstones, with cross stratification, interbedded with finely laminated purple and green mudrocks and thin pyroclastic levels (Harrington, 1947, 1970; Andreis et al., 1979; Andreis and Cladera, 1992; Zavala et al., 1993, 2019; López-Gamundí et al., 1995; Arzadún et al., 2018). There are many uncertainties regarding its thickness due to the lithological homogeneity and tectonic complexity, and the absence of marker horizons. The exposed thickness ranges from 600 m to 2400 m (Harrington, 1970; Suero, 1972; Andreis and Japas, 1991; Vazquez Lucero et al., 2020). In the subsurface of the Claromecó Basin, this unit reaches 700 m in thickness (Lesta and Sylwan, 2005; Zorzano et al., 2011; Arzadún et al., 2017). The *Glossopteris* flora indicates an Early Permian age (Sakmarian–Artinskian; Archangelsky and Cúneo, 1984), which is consistent with the U–Pb zircon ages (284 ± 15 Ma, Alessandretti et al., 2013; 282.4 ± 2.8 Ma, Tohver et al., 2008; 280.8 ± 1.9 Ma, López-Gamundí et al., 2013) obtained from pyroclastic layers located at Abra del Despeñadero (top of the sequence; Figs. 1B and 2A). Recently, Ballivián Justiniano et al. (2020) proceeded LA–ICP–MS U–Pb zircon dating from tuff layers, obtaining ages between 314 Ma and 289 Ma at Las Mostazas locality (top of the sequence; Figs. 1B and 2A). Arzadún et al. (2018) obtained SHRIMP U–Pb zircon ages of 291.7 ± 2.9 Ma from tuff layers located at Ruta 76 (base of the sequence; Figs. 1B, 2A) and 295.5 ± 8.0 Ma from the PANG 0001 well (Fig. 3). These ages are consistent with available palynological data from core samples of the Tunas Formation (di Pasquo et al., 2018).

Cores of the Tunas Formation were recovered from wells PANG 0001 ($S37^{\circ}40.8'17''$, $W61^{\circ}11'30.06''$) and PANG 0003 ($S37^{\circ}34'44.24''$, $W61^{\circ}22'12.56''$) located in the northwest of the Claromecó Basin (Fig. 1), which are preserved and stored at Universidad Nacional del Sur, Bahía Blanca, Argentina. Sediments are composed of medium- to fine-grained sandstones, with black organic-rich mudrocks, heterolites, greenish mudrocks, tuff levels, carbonaceous mudrocks and coal levels (Zorzano et al., 2011; Arzadún et al., 2016a, 2017; Febbo et al., 2017, 2018a; Zavala et al., 2019; this work).

3. Provenance and tectonic evolution of the Pillahuincó Group

The Upper Paleozoic deposits of the Pillahuincó Group represent the onset of the foreland stage in

the evolution of the Claromecó Basin (Ramos, 1984; López-Gamundí and Rossello, 1992; López-Gamundí et al., 1995). The paleotectonic scenario changed between the deposition of the lower units (Sauce Grande, Piedra Azul and Bonete formations) and the uppermost unit (Tunas Formation). The oldest units are characterized by quartz-rich petrofacies, with bimodal paleocurrents from ENE–WSW, which indicate a cratonic source area (Fig. 2B; Andreis and Cladera, 1992; López-Gamundí et al., 1995). On the other hand, lithic-rich petrofacies and inversion in the paleocurrent directions, coming from SW, denote a recycled orogen/magmatic arc source area for the Tunas Formation (Fig. 2B; Andreis and Cladera, 1992; López-Gamundí et al., 1995; López-Gamundí and Rossello, 1998; Alessandretti et al., 2013; Ramos and Naipauer, 2014; Ballivián Justiniano et al., 2020).

The Tunas Formation was interpreted as a synorogenic unit, based on the occurrence of growth strata (López-Gamundí et al., 1995, 2013) and paleomagnetic data that show syntectonic magnetizations acquired during or very soon after its deposition (Tomezzoli, 1999, 2001; Tomezzoli and Vilas, 1999). The sedimentation was contemporary with the explosive volcanic activity evidenced by tuffs interbedded with clastic material (Fig. 2), which confirms an Early Permian volcanism in the southwestern Gondwana margin (Alessandretti et al., 2013; López-Gamundí et al., 2013; Arzadún et al., 2018; Ballivián Justiniano et al., 2020). These events are interpreted as the distal equivalent of the earliest Choiyoi volcanic episodes in western Argentina (López-Gamundí, 2006; López-Gamundí et al., 2013; Sato et al., 2015).

4. Methodology

Petrographic and modal composition analyses were performed on 30 sandstone samples from the Tunas Formation: 22 samples from the subsurface (PANG 0001 and PANG 0003 wells; Fig. 3) and 8 samples from the outcrop (Gonzales Chaves locality; Fig. 4) at the Claromecó Basin center. The sedimentary sequences for PANG 0001 and PANG 0003 boreholes can reach depths of ~900 meters below wellhead (mbw), and are overlayed by Cenozoic deposits with a thickness of ~180 m.

Petrographic studies were performed with a Nikon Eclipse 50i POL microscope. The modal composition was determined according to the Gazzi-Dickinson method, counting 300–350 grains per

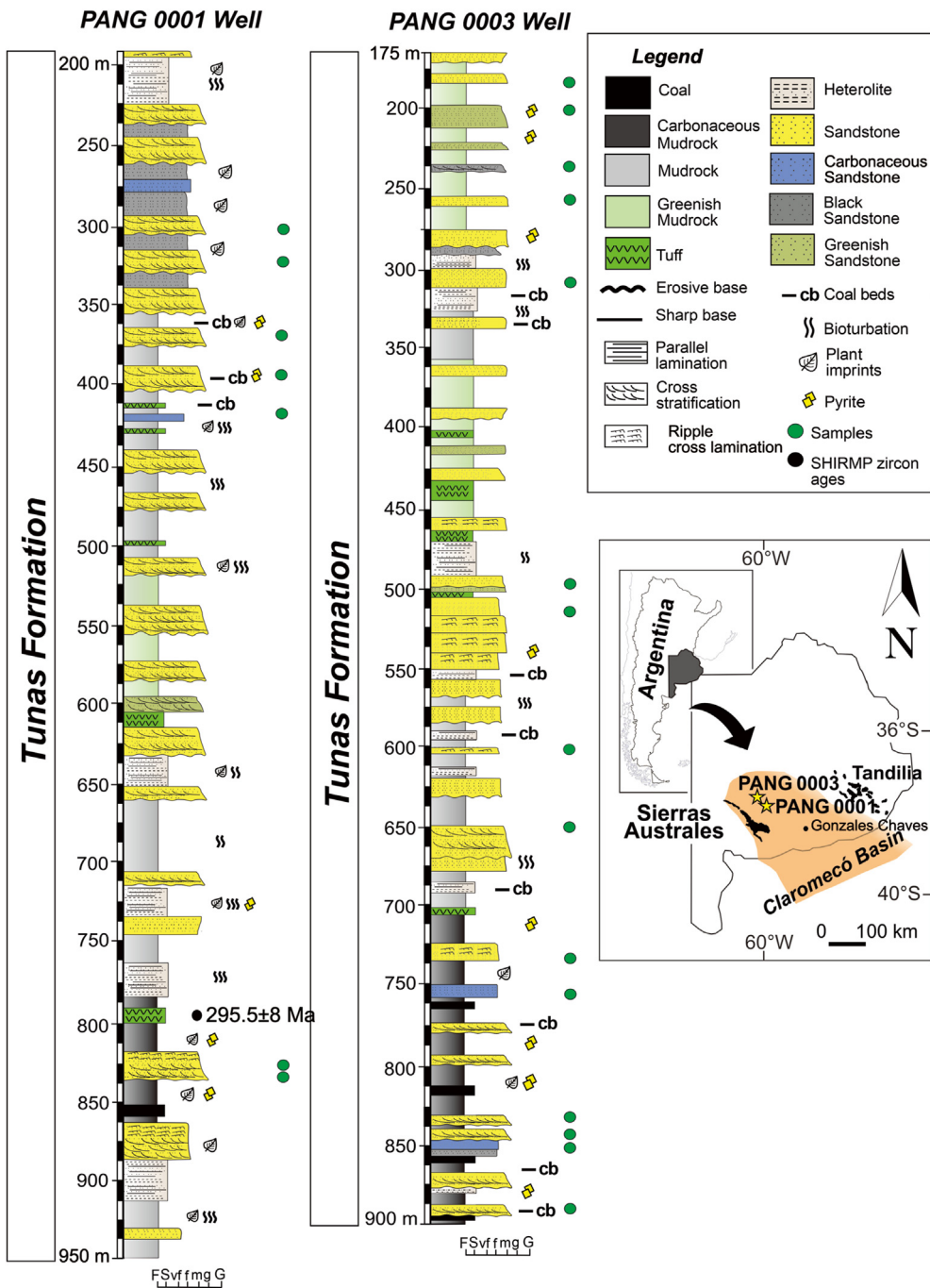


Fig. 3 Sedimentary logs of the Tunas Formation in PANG 0001 and PANG 0003 wells, showing the location of analyzed sandstones samples, SHIRMP zircon ages obtained by Arzadún *et al.* (2018) and studied wells.

sample. This method minimizes the compositional variability due to the influence of grain size (Dickinson, 1970; Ingersoll *et al.*, 1984; Zuffa *et al.*, 1995). Sandstone constituents were classified into monocrystalline quartz (Qm), polycrystalline quartz (Qp), potassium feldspars (Fk), plagioclase (Pl) and lithic fragments that include volcanic (Lv) and sedimentary and metasedimentary (Ls-m) ones. They

were differentiated based on optical mineralogical characteristics, such as extinction, twinning and relict textures. Sandstones were classified according to Folk *et al.* (1970) based on their quartz, feldspar and lithic content, recalculated to 100% (Table 1). Detrital constituents in the framework, percentage of matrix, porosity and cement were visually estimated by microscopic analysis.

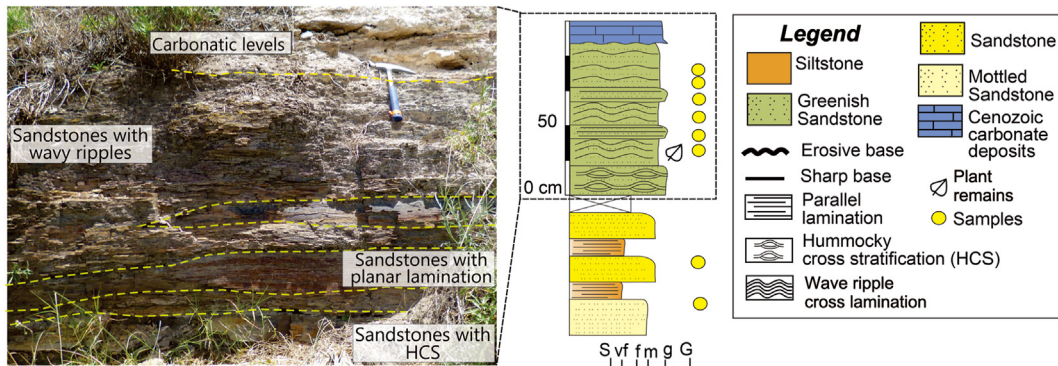


Fig. 4 Outcrops and sedimentary log of the Tunas Formation at the Gonzales Chaves locality, showing the location of analyzed sandstones samples.

Ternary diagrams QFL (total quartz–feldspars–lithic fragments) and QmFLt (monocrystalline quartz–feldspars–total lithic fragments + polycrystalline quartz), proposed by [Dickinson et al. \(1983\)](#), were used to determine provenance sources ([Table 2](#)). QmPLK

complementary diagrams were employed to differentiate the crystalline basement supply from that of the volcanic arc ([Table 2](#)). In addition, results were compared with the Tunas Formation outcrop data from the Sierras Australes area obtained by other authors

Table 1 Main features of the Tunas Formation sandstones and their classification based on Folk *et al.* (1970). The summary of the major detrital components was recalculated to 100%.

	Sample	Depth	QFL (%)			Folk <i>et al.</i> (1970)'s classification
			Q	F	L	
PANG 0001 Well	509	304.6	48.7	15.3	36.0	Feldspathic litharenite
	495	323.2	44.6	14.5	40.9	Feldspathic litharenite
	458	365.6	47.7	7.4	44.9	Litharenite
	442	382.5	38.0	14.3	47.7	Litharenite
	414	419.3	43.5	7.0	49.5	Litharenite
	103a	822.8	46.9	9.4	43.7	Litharenite
	103b	821.5	44.5	10.5	45.0	Litharenite
PANG 0003 Well	M377	182.4	55.0	15.0	30.0	Feldspathic litharenite
	M368	198.9	54.5	15.4	30.1	Feldspathic litharenite
	M351	239.6	51.3	16.5	32.2	Feldspathic litharenite
	M343	251.5	48.2	13.6	38.2	Feldspathic litharenite
	M315	311.5	40.9	21.5	37.6	Feldspathic litharenite
	M261	492.6	42.5	15.5	42.0	Feldspathic litharenite
	M248	516.3	51.0	17.0	32.0	Feldspathic litharenite
	M212	601.0	53.5	20.5	26.0	Feldspathic litharenite
	M186	648.9	57.8	13.3	28.9	Feldspathic litharenite
	M136	732.0	41.0	10.9	48.1	Litharenite
	M117	757.2	50.0	9.4	40.6	Litharenite
	M54	838.3	43.6	16.4	40.0	Feldspathic litharenite
	M47	846.3	44.6	7.0	48.4	Litharenite
	M38	854.8	54.2	10.8	35.0	Litharenite
	M22	879.9	43.0	12.5	44.5	Litharenite
Gonzales Chaves	G Ch1	Outcrop	54.0	8.8	37.2	Litharenite
	G Ch2	Outcrop	57.2	8.8	34.0	Litharenite
	G Ch3	Outcrop	47.0	16.4	36.6	Litharenite
	P2	Outcrop	51.5	14.0	34.5	Feldspathic litharenite
	P4	Outcrop	51.4	9.8	38.8	Litharenite
	Gh 00	Outcrop	42.8	16.0	41.2	Feldspathic litharenite
	Gh 01	Outcrop	48.0	18.6	33.4	Feldspathic litharenite
	Gh 02	Outcrop	47.1	18.3	34.6	Feldspathic litharenite

F: Feldspars; L: Lithic fragments; Q: Quartz.

Table 2 Detrital modes from Tunas Formation sandstones (recalculated 100%).

	Sample	Qm	Qp	K	Pl	Lv	Ls	Dickinson et al. (1983)			Dickinson and Suczek (1979)		
								QFL (%)			QmFLt (%)		
								Q	F	L	Qm	F	Lt
PANG 0001 Well	509	40.1	8.6	5.3	10.0	27.2	8.8	48.7	15.3	36.0	40.1	15.3	44.6
	495	36.6	8.0	4.0	10.5	30.0	10.9	44.6	14.5	40.9	36.6	14.5	48.9
	458	46.6	1.1	1.7	5.7	10.9	34.0	47.7	7.4	44.9	46.6	7.4	46.0
	442	36.0	2.0	9.5	4.8	22.7	25.0	38.0	14.3	47.7	36.0	14.3	49.7
	414	41.8	1.7	2.2	4.8	11.9	37.6	43.5	7.0	49.5	41.8	7.0	51.2
	103a	42.5	4.4	1.9	7.5	18.0	25.7	46.9	9.4	43.7	42.5	9.4	48.1
	103b	43.4	1.1	2.7	7.8	10.9	34.1	44.5	10.5	45.0	43.4	10.5	46.1
	M377	50.0	5.0	3.8	11.2	18.5	11.5	55.0	15.0	30.0	50.0	15.0	35.0
PANG 0003 Well	M368	43.1	11.4	6.8	8.6	19.0	11.1	54.5	15.4	30.1	43.1	15.4	41.5
	M351	43.7	7.6	3.5	13.0	23.5	8.7	51.3	16.5	32.2	43.7	16.5	39.8
	M343	44.8	3.4	3.4	10.2	23.2	15.0	48.2	13.6	38.2	44.8	13.6	41.6
	M315	37.2	3.7	8.7	12.8	22.2	15.4	40.9	21.5	37.6	37.2	21.5	41.3
	M261	32.8	9.7	2.2	13.3	25.2	16.8	42.5	15.5	42.0	32.8	15.5	51.7
	M248	42.3	8.7	4.5	12.5	19.4	12.6	51.0	17.0	32.0	42.3	17.0	40.7
	M212	43.7	9.8	6.9	13.6	14.5	11.5	53.5	20.5	26.0	43.7	20.5	35.8
	M186	50.3	7.5	4.8	8.5	13.0	15.9	57.8	13.3	28.9	50.3	13.3	36.4
	M136	40.2	0.8	2.9	8.0	17.6	30.5	41.0	10.9	48.1	40.2	10.9	48.9
	M117	46.8	3.2	1.9	7.5	15.1	25.5	50.0	9.4	40.6	46.8	9.4	43.8
	M54	42.6	1.0	2.4	14.0	9.6	30.4	43.6	16.4	40.0	42.6	16.4	41.0
	M47	37.6	7.0	1.1	5.9	13.4	35.0	44.6	7.0	48.4	37.6	7.0	55.4
	M38	54.0	0.2	3.3	7.5	5.0	30.0	54.2	10.8	35.0	54.0	10.8	35.2
	M22	37.0	6.0	5.5	7.0	11.4	33.1	43.0	12.5	44.5	37.0	12.5	50.5
	GChi1	51.0	3.0	2.0	6.8	10.2	27.0	54.0	8.8	37.2	51.0	8.8	40.2
	GChi2	42.2	15.0	3.3	5.5	15.5	18.5	57.2	8.8	34.0	42.2	8.8	49.0
	GChi3	37.6	9.4	2.4	14.0	15.5	21.1	47.0	16.4	36.6	37.6	16.4	46.0
	P2	46.0	5.5	2.3	11.7	9.7	24.8	51.5	14.0	34.5	46.0	14.0	40.0
Gonzales Chaves	P4	48.0	3.4	2.8	7.0	10.5	28.3	51.4	9.8	38.8	48.0	9.8	42.2
	Gh 00	38.4	4.4	3.1	12.9	2.7	38.5	42.8	16.0	41.2	38.4	16.0	45.6
	Gh 01	41.8	6.2	3.9	14.7	6.4	27.0	48.0	18.6	33.4	41.8	18.6	39.6
	Gh 02	38.9	8.2	2.0	16.3	5.0	29.6	47.1	18.3	34.6	38.9	18.3	42.8

F: Feldspars (K + Pl); K: Potassium feldspar; L: Total lithic fragments (Ls + Lv); Ls: Sedimentary/metasedimentary lithic fragments; Lt: Total lithic fragments + polycrystalline quartz (L + Qp); Lv: Volcanic lithic fragments; Pl: Plagioclase; Q: Total quartz; Qm: Monocrystalline quartz; Qp: Polycrystalline quartz.

(Andreis and Cladera, 1992; López-Gamundí *et al.*, 1995; Alessandretti *et al.*, 2013; Ballivián Justiniano *et al.*, 2020).

5. Results

5.1. Sandstone petrography

Petrographic and modal analyses were performed on the Tunas Formation samples from subsurface (Fig. 3; PANG 0001 and PANG 0003 wells) and outcrops (at the Gonzales Chaves locality; Fig. 4). The subsurface sequences are composed of carbonaceous mudrocks and coal beds with abundant pyrite nodules, plant remains and *Glossopteris* imprints, which are interbedded with medium- to fine-grained grayish sandstones. Coal beds have a thickness of 0.5 m–4 m. Towards the top, the sequences are dominated by

medium- to fine-grained greyish to greenish sandstones, greenish mudrocks and heterolites interbedded with thin tuffs and coal beds (Fig. 3).

The sedimentary succession outcropping in Gonzales Chaves locality (Fig. 1A) is characterized by small outcrops (<2 m in thickness) composed of fine-grained brownish mottled sandstones interbedded with laminated mudrocks (Fig. 4). Towards the top, the succession is dominated by medium- to fine-grained greenish sandstones with planar lamination, interbedded with fine- to very fine-grained sandstones with wave ripples cross lamination (Fig. 4). Upwards, the succession is overlain by Cenozoic carbonate deposits (Fig. 4).

Sandstones were classified as feldspathic litharenites (53%) and litharenites (47%) according to Folk *et al.* (1970) (Table 1; Fig. 5). The average modal composition is Q49 F13 L38, showing scarce variations along the analyzed sequence. Grain size varies from

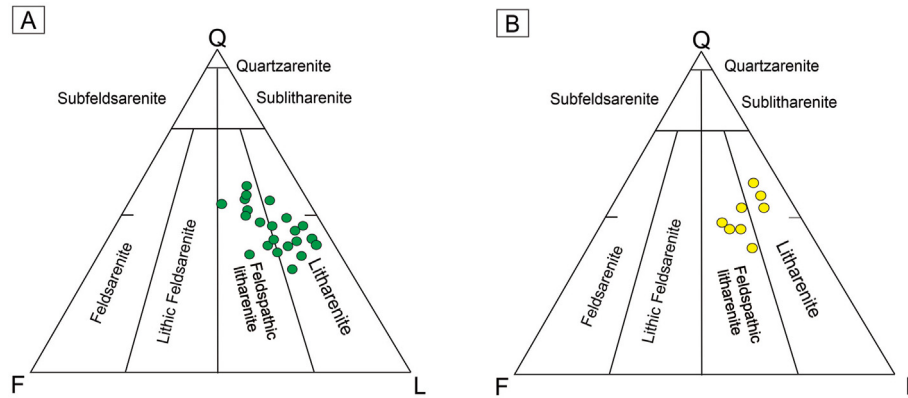


Fig. 5 Classification diagram according to [Folk et al. \(1970\)](#) for the Tunas Formation sandstones from A) Subsurface samples (PANG 0001 and PANG 0003 wells); B) Outcrop samples (Gonzales Chaves locality). Q: Quartz, F: Feldspar, L: Lithic fragments.

medium (1 mm) to very fine (0.062 mm), predominating medium to fine grain sizes. Sandstones are clast-supported, with sub-rounded to sub-angular grains, long to concavo-convex contacts and moderate-to-well sorting.

Quartz, feldspar and lithic fragments dominate sandstone framework components. Quartz occurs as monocrystalline or polycrystalline grains, constituting from 38% to 57.8% of the total main components ([Tables 1 and 2](#)). Monocrystalline quartz predominates, with an average of 43.25% ([Table 2](#)). Grains have sub-rounded to sub-angular shapes with straight and occasionally undulatory extinction ([Fig. 6A and B](#)). Polycrystalline quartz is scarce, with an average of 5.5% ([Table 2](#)). Grains show sub-angular shapes ([Fig. 6C](#)).

Feldspars include potassium feldspar and plagioclase, comprising from 7% to 21.5% of the total main components ([Tables 1 and 2](#)). Plagioclase predominates, with an average of 9.2% ([Table 2](#)). Grains usually exhibit polysynthetic twinning and sub-tabular shapes ([Fig. 6D and E](#)). Potassium feldspar is represented by orthoclase and microcline, with an average of 3.7% ([Table 2](#)). The orthoclase is usually untwinned, with sub-tabular shapes ([Fig. 6D](#)). Microcline exhibits tartan twinning, with sub-tabular shapes ([Fig. 6F](#)). The plagioclase to total feldspar (Pl/Ft) ratio ranges from 0.85 to 0.60 with an average of 0.70.

Lithic fragments include metamorphic, sedimentary and volcanic rock fragments, constituting from 26% to 49.7% of the total main components ([Tables 1 and 2](#)), with an average of 35.8%. Metamorphic and sedimentary rock fragments are dominant at the basal and middle portion of the succession, while volcanic ones increase in content toward the uppermost part ([Table 2](#)). Metamorphic lithic fragments have a low to medium metamorphic grade, comprising shales,

slates, schists and quartzites ([Fig. 6B and E](#)). Grains show sub-angular shapes. Sedimentary rock fragments include claystones, siltstones and very-fine sandstones, with sub-angular to sub-rounded shapes ([Fig. 6E and G](#)). Volcanic fragments present microlithic and vitrophyric textures ([Fig. 6H and I](#)) of sub-rounded shapes.

Accessory minerals comprising from 0.1% to 3% of the total main components, consist of micas (muscovite, biotite, and chlorite; [Fig. 6J](#)), sulfurs (commonly pyrite; [Fig. 6K and L](#)), epidote and undetermined opaque minerals. Samples also present dispersed organic matter ([Fig. 6K](#)).

Sandstones have low matrix content (<5%), composed of quartz, lithic rock fragments and clay minerals. The presence of pseudomatrix is common, formed by unstable detrital grains. Cement constitutes 5%–15% of the total rock volume, composed of carbonate, zeolite (laumontite), quartz and feldspar. Authigenic minerals, such as calcite, zeolite, and clay minerals, often replaced framework grains, especially feldspar and lithic fragments. It should be noted that diagenetic processes affected the unstable components of the framework (especially feldspar and lithic fragments), making it difficult to differentiate them.

5.2. Provenance analysis

Sandstone modal composition of the Tunas Formation from the subsurface (PANG 0001 and PANG 0003 wells) and outcrops was plotted on the QFL and QmFLT ternary diagrams of [Dickinson et al. \(1983\)](#) and on the QmPlK complementary diagram of [Dickinson and Suczek \(1979\)](#) ([Table 2; Fig. 7](#)) to determine tectonic provenance. In the QFL diagram, samples from subsurface and outcrops are located in the recycled orogen field ([Fig. 7A](#)). In the QmFLT diagram, samples

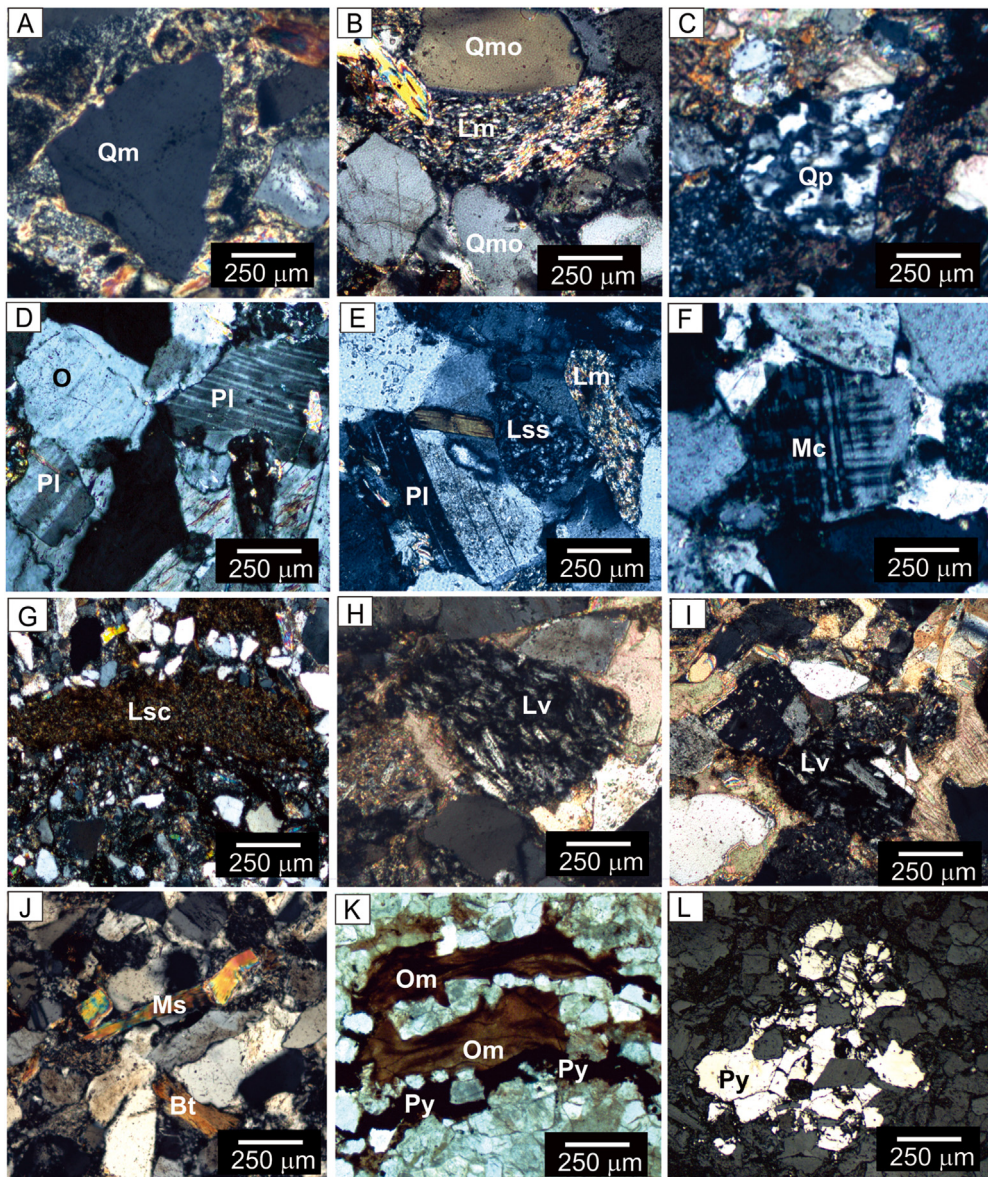


Fig. 6 Thin-section photomicrographs of modal components for Tunas Formation sandstones. A) Monocrystalline quartz with straight extinction (Qm); B) Monocrystalline quartz with undulatory extinction (Qmo) and metamorphic lithic fragment (Lm); C) Polycrystalline quartz (Qp); D) Orthoclase (O) and plagioclase (Pl); E) Plagioclase (Pl), sandstone lithic fragment (Lss) and metamorphic lithic fragment (Lm); F) Microcline (Mc) with tartan twining; G) Mudrock lithic fragment (Lsc); H) Volcanic lithic fragment (Lv) with microlitic texture; I) Volcanic lithic fragment (Lv) with vitphyric texture; J) Muscovite (Ms) and biotite (Bt); K) Organic matter (Om) and associated pyrite (Py); L) Pyrite (Py). Photomicrographs are taken under transmitted light with crossed Nicols (A–K) and under reflected light (L).

from subsurface correspond to the basal and middle portion of the sequence lay in the transitional recycled field, while those from the top of the sequence fall in the mixed field (Fig. 7B). This difference is due to a slight increase in feldspar content towards the upper portion of the succession (see Table 2). Similarly, samples from outcrops are located in the transitional recycled to mixed fields (Fig. 7B).

In the QmPIK complementary diagram, most of samples fall in the upper part, which reveals a high

content of quartz and a minor proportion of plagioclase (Fig. 7C), representing a recycled orogen source (or provenance from continental blocks) according to Dickinson and Suczek (1979). However, samples from subsurface belonging to the top of the sequence are slightly enriched in plagioclase, probably associated with a volcanic source (Fig. 7C). The content of K-feldspar is low; only a few subsurface samples show a similar range of K-feldspar and plagioclase (Fig. 7C).

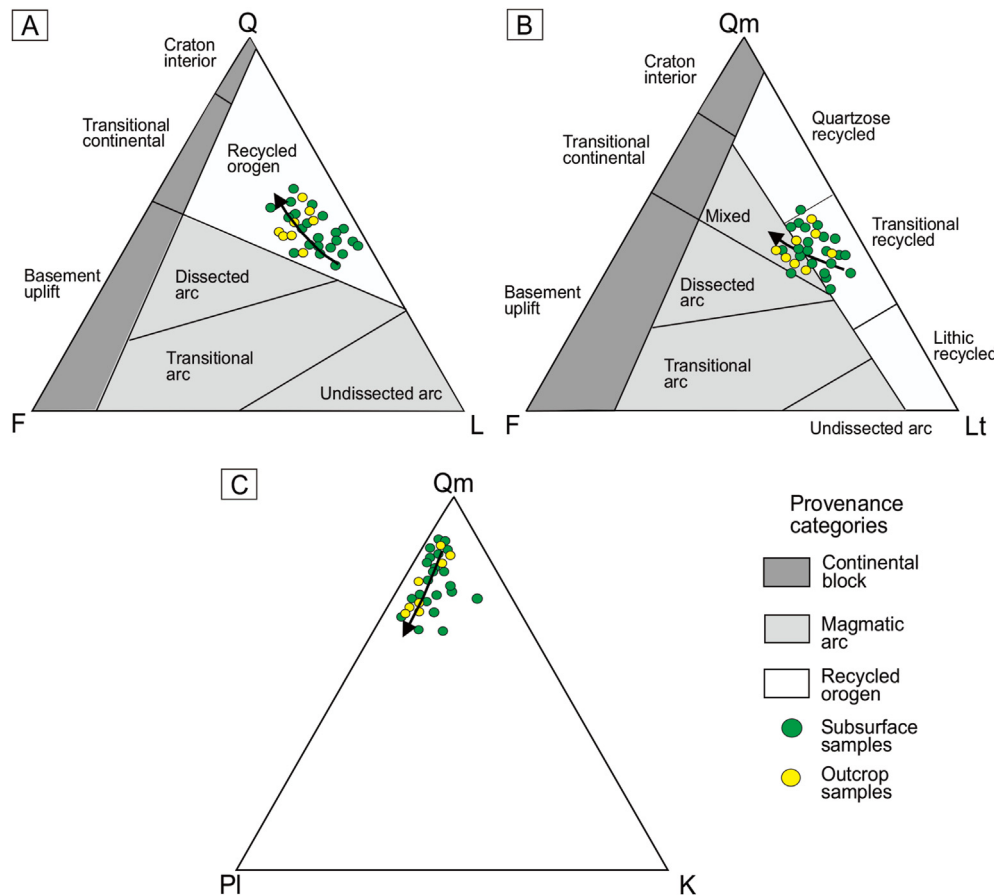


Fig. 7 QFL, QmFLt and QmPLK diagrams with provenance areas according to Dickinson et al. (1983) for Tunas Formation sandstones from subsurface (PANG 0001 and PANG 0003 wells, green circles) and outcrops (Gonzales Chaves locality, yellow circles). A) QFL discrimination diagram, B) QmFLt discrimination diagram with provenance areas according to Dickinson et al. (1983), and C) QmPLK discrimination diagram of Dickinson and Suczek (1979). Arrows show the evolution from the lower towards the upper part of the analyzed succession. Q: Total quartz grains; F: Feldspars ($K + Pl$); L: Total lithic fragments ($Ls + Lv$); Qm: Monocrystalline quartz; Pl: Plagioclase; K: Potassium feldspar.

6. Discussion

Sandstone modal composition from different basins is a function of diverse provenance areas governed by plate tectonics (Dickinson and Suczek, 1979). In addition, the composition of detrital constituents from sedimentary rocks is also influenced by paleoclimate, weathering, transport agents and mechanism, distance from source area, depositional environment, and diagenesis (Dickinson and Suczek, 1979; McBride, 1985; DeCelles and Hertel, 1989). In foreland basins, the sedimentary supply is linked to the adjacent orogenic belt evolution (Dickinson and Suczek, 1979; Dickinson et al., 1983; DeCelles, 1986; DeCelles and Hertel, 1989). In the case of the Sierras Australes fold and thrust belt and the adjacent Claromecó Basin, the tectonic evolution is complex and recorded multiple compressional (Arzadún et al., 2021) and extensional events throughout the Paleozoic–Mesozoic

(Lovechio et al., 2018, 2020; Arzadún et al., 2020). Provenance studies of the synorogenic deposits of the Tunas Formation constitute a key piece to understand the paleotectonic context during the last filling stage of the Claromecó Foreland Basin and to reconstruct the uplift history of the Sierras Australes fold and thrust belt.

6.1. Provenance areas for the Tunas Formation

The results obtained from petrography analyses of Tunas Formation sandstones reveal a high proportion of metamorphic and volcanic components, which suggest mixed provenance areas. Monocrystalline quartz and lithic fragments (mainly metamorphic and volcanic) dominate the main proportion of the framework clasts, while feldspar content is subordinate (Table 2). The presence of sub-angular to sub-rounded clasts, products of low to moderate sediment transport, could

indicate source areas located close to the basin. Monocrystalline quartz with undulatory extinction, polycrystalline quartz grains and metamorphic and sedimentary lithics could be derived from the weathering of metamorphic and/or sedimentary rocks, related to the fold-thrust belt erosion. Detrital feldspar grains could be supplied by metamorphic and volcanic rocks (Datta, 2005). The relatively high values of the plagioclase to total feldspar ratio (>0.60) indicate a mixture of volcanic and metamorphic sources (Dickinson, 1970). Volcanic lithic fragments of acid and intermediate composition, with characteristic features of neo-volcanic fragments (Critelli and Ingersoll, 1995) and tuff layers interbedded with the siliciclastic sequence (Fig. 3), indicate volcanic explosive events coetaneous with sedimentation. Moreover, zeolites, occurred as cement or detrital grains, could be related to alteration and replacement of volcanic materials (De Ros *et al.*, 1997; Morad *et al.*, 2010).

Tectonic provenance analysis for the Tunas Formation sandstones defines a sedimentary material supplied from a mixed provenance source, contributed by the recycled orogen and magmatic arc (Fig. 7). These results, in addition to paleocurrent dataset, coming from the southwest (Andreis and Japas, 1991; López-Gamundí *et al.*, 1995), suggest a sedimentary material contribution potentially linked to the Sierras Australes fold and thrust belt, located to the W/SW, adjacent to the Claromecó Basin (Fig. 1). Polycrystalline quartz grains and abundant metamorphic lithics in sandstone constituents (Andreis and Cladera, 1992; López-Gamundí *et al.*, 1995; this study), propose an adjacent uplifted orogenic belt (Sierras Australes), which supplied material to the basin from the recycled orogen. Metamorphic and sedimentary components could be derived from quartzites of the Mascota, Tucumán, Napostá or Providencia formations (Curamalal and Ventana Groups; Fig. 1B) and slates and schists corresponding to the Lolén Formation (Ventana Group; Fig. 1B).

The sedimentation was coeval with volcanic activity, recorded by the intercalation of pyroclastic material (tuff beds) and sandstones with significant amounts of volcanic lithics. The increase in volcanic components upwards in the sequence suggests that volcanic material contribution was relevant towards the final stages of the Tunas Formation deposition (Table 2). Tuff layers are present in Tunas Formation outcrops (Figs. 1B and 2A; e.g., Ruta 76: Arzadún *et al.*, 2018; Abra del Despeñadero: Iñíguez *et al.*, 1988; López-Gamundí *et al.*, 1995, 2013; Alessandretti *et al.*, 2013; and Las Mostazas: Ballivián Justiniano *et al.*, 2020) and in the subsurface (PANG 0001 and 0003 wells, Fig. 3; Arzadún *et al.*, 2018,

2020). These pyroclastic levels with an Artinskian age (average of 285.5 ± 2.4 Ma; Ballivián Justiniano *et al.*, 2020 and references therein) confirm the existence of an active Early Permian pyroclastic activity along southwestern Gondwana margin. Volcanic events have been interpreted as the earliest episodes of the Choioyi volcanism in western Argentina (Rocha-Campos *et al.*, 2011; Alessandretti *et al.*, 2013; López-Gamundí *et al.*, 2013; Sato *et al.*, 2015) and have been reported in other Permian Gondwana basins as the Paraná (Brazil) and Karoo (South Africa) basins (Bangert *et al.*, 1999; Stolhofen *et al.*, 2000; Guerra-Sommer *et al.*, 2005; Rocha-Campos *et al.*, 2006, 2008). Based on magmatic detrital zircon ages, Ramos and Naipauer (2014) interpreted the volcanic material as derived from a Lower Paleozoic magmatic arc, located to the south, in the North Patagonian Massif. Other authors (e.g., Sato *et al.*, 2015; Ballivián Justiniano *et al.*, 2020) argued that the pyroclastic material could have been supplied from the Chilean Precordillera, Frontal Cordillera and Las Matras and Chadileuvú blocks, related to the Choioyi magmatic province, located to the W–SW–S.

The results of this work are slightly different from those obtained by other authors for the Tunas Formation outcrops of the Sierras Australes fold and thrust belt area (Fig. 8). In the QmFLt diagram, subsurface and outcrop samples (Claromecó Foreland Basin area, this study) are distributed into transitional recycled to mixed fields, while outcrop samples (Sierra Australes area; Andreis and Cladera, 1992; López-Gamundí *et al.*, 1995; Alessandretti *et al.*, 2013; Ballivián Justiniano *et al.*, 2020) show more feldspar-rich, falling into the mixed to dissected arc fields (Fig. 8). These differences are mainly due to feldspar content. Variations in sandstone composition could be attributed to different transport distances from the provenance area (Sierras Australes) to the basin center (PANG 0001 and 0003 wells and Gonzales Chaves locality), during which feldspars could be eroded by mechanical transportation. Furthermore, diagenetic processes, such as alteration, dissolution, and replacement, affected unstable framework components like feldspar and lithic fragments, and could influence detrital mode determinations.

6.2. Paleotectonic implications

Differences in provenance areas between the lower (Sauce Grande, Piedra Azul and Bonete formations; Fig. 2) and the uppermost (Tunas Formation; Fig. 2) units of the Pillahuincó Group were the consequence of variations in basin configuration during the Late Carboniferous–Early Permian. Quartz-rich petrofacies

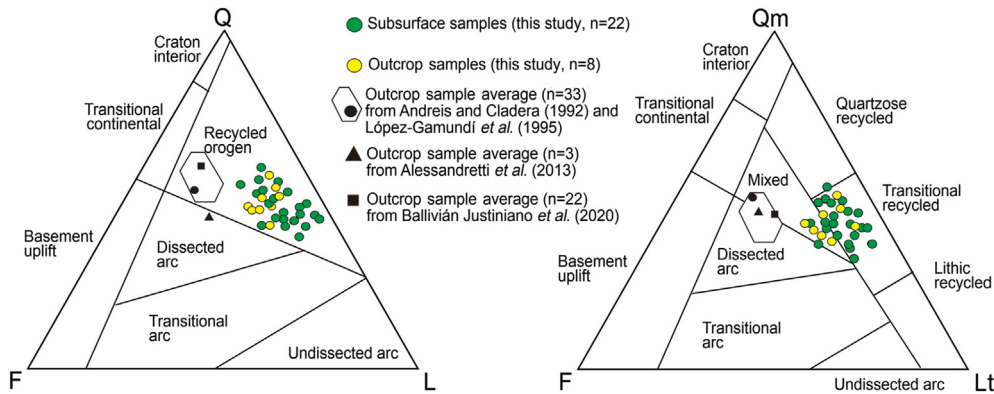


Fig. 8 QFL and QmFLT diagrams with provenance areas according to Dickinson *et al.* (1983) for Tunas Formation sandstones from Claromecó Basin area (this study; green and yellow circles) and from outcrops (black circles, triangles and squares) in the Sierras Australes fold and thrust belt obtained by Andreis and Cladera (1992), López-Gamundi *et al.* (1995), Alessandretti *et al.* (2013) and Ballivián Justiniano *et al.* (2020). Results from the Claromecó Basin area are distributed into recycled orogen and transitional recycled/mixed fields, while data from the Sierras Australes fold and thrust belt fall in the recycled orogen and mixed to dissected arc fields.

and bimodal paleocurrents, from ENE–WSW, suggest a cratonic source area for Sauce Grande, Piedra Azul and Bonete formations (Fig. 2B; Andreis and Cladera, 1992). Sediment supply may be attributed to quartzites from the Ventana Group (e.g., Naposta and Providencia Formations), exposed along the western portion of the Sierras Australes fold and thrust belt (Fig. 1). Oppositely, lithic-rich petrofacies and inversion in paleocurrent direction from SW denote mixed source for the Tunas Formation (Figs. 7 and 8). These changes in the paleotectonic setting were the result of a compressive post-collisional deformation occurred along the southwestern Gondwana margin, the product of the adjustment and accommodation of previously collided terrains, and the translation of landmasses towards the equator to form Pangea during the Late Permian–Triassic (Fig. 9; Tomezzoli, 2001, 2012).

Changes in paleotectonic and paleogeographic settings are also evidenced by paleoenvironmental and paleoclimatic conditions during the deposition of the Pillahuincó Group. As a consequence, there is a clear transition from the shallow marine conditions during the depositional period of the Piedra Azul and Bonete formations (Harrington, 1970; Andreis *et al.*, 1989) to deltaic and fluvial conditions represented by the Tunas Formation deposits (Andreis *et al.*, 1989; Zavala *et al.*, 1993, 2019; López-Gamundi *et al.*, 1995; Andreis and Japas, 1996). A continentalization of the basin occurred as a result of the deformation and uplift of the Sierras Australes fold and thrust belt, with development of continental to mixed environments. Towards the foreland basin area, the presence of floodplains and interdistributary swamps (Arzadún

et al., 2016a, 2017; Zavala *et al.*, 2019) promoted the accumulation and preservation of organic matter in coal-bearing deposits (PANG 0001 and PANG 0003 wells; Fig. 3). The development of carbonaceous deposits reveals an improvement in climate conditions during the Late Paleozoic, characterized by cold and humid weather (Limarino *et al.*, 2014; Arzadún *et al.*, 2017; Gallo *et al.*, 2020), resulting from the Gondwana supercontinent drift across the South Pole towards high paleolatitudes (Tomezzoli *et al.*, 2018; Gallo *et al.*, 2020, Fig. 9).

The deformation and uplift of the Sierras Australes fold and thrust belt were linked to different tectonic events. For some authors, the Earl Paleozoic Gondwanides Orogeny (Permian–Triassic; Keidel, 1916; Du Toit, 1927; Milani and De Wit, 2008), known as San Rafaelic orogenic phase in Argentina (SROPh; Azcuy and Caminos, 1987) and Hercinian phase in the rest of Gondwana, was responsible for the construction and configuration of fold and thrust belts in South America (Sierras Australes; Ramos, 1984, 2008; Págaro and Ramos, 2012) and South Africa (Cape Fold System; De Wit *et al.*, 1988; Catuneanu *et al.*, 1998). These compression events were not exclusive to the southwest Gondwana margin, by contrary, they were recorded along all the southern margin of Gondwana during the Permian (e.g., Catuneanu *et al.*, 1998). For other authors, the tectonic deformation began in the Late Devonian–Early Carboniferous (Cháñica orogenic phase in Argentina, ChOPh; Azcuy and Caminos, 1987) as a consequence of terrane collision against Gondwana from the west and the south (Chilenia terrane and Patagonia terrane respectively, i.e., CHI–PA; Tomezzoli *et al.*, 2019), and continued until the

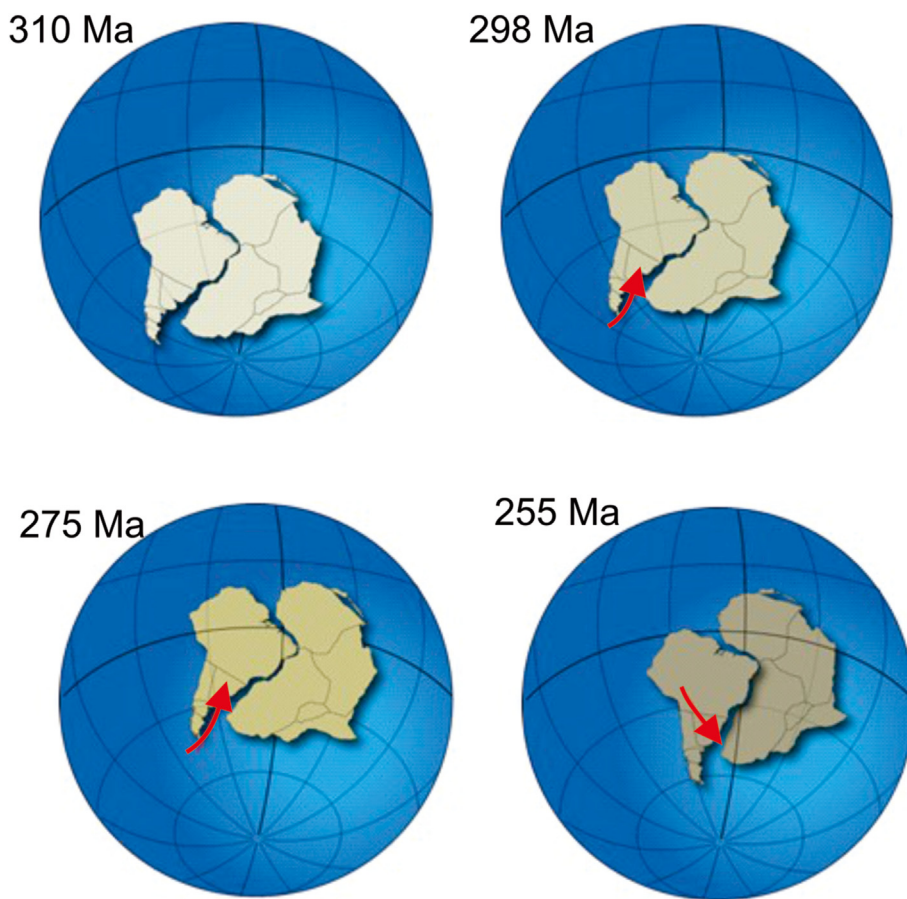


Fig. 9 Paleogeographic reconstruction of the Gondwana supercontinent during the Late Paleozoic showing latitudinal movements of continents toward the equator during the Permian (red arrows), based on paleomagnetic poles of Tomezzoli (2009) and Gallo *et al.* (2017). Modified from Arzadún *et al.* (2017).

Permian (Tomezzoli, 2001, 2012). This Permian deformation was recorded in the Tunas Formation by the occurrence of synorogenic deposits (López-Gamundi *et al.*, 1995, 2013) and changes in provenance areas (Andreis and Cladera 1992; López-Gamundi *et al.*, 1995; Alessandretti *et al.*, 2013; Ramos and Naipauer, 2014; Ballivián Justiniano *et al.*, 2020; this work). In addition, Permian deformation was also recorded by different types of paleomagnetization (Tomezzoli and Vilas, 1999; Tomezzoli, 2001), anisotropy of magnetic susceptibility (Arzadún *et al.*, 2017, 2021; Febbo *et al.*, 2021), and structural data (Tomezzoli and Cristallini, 1998). Recent anisotropy of magnetic susceptibility results (Arzadún *et al.*, 2021) obtained all along the Pillahuincó Group show that during the Late Paleozoic the tectonic deformation had a spasmodic behavior, with cycles of higher and lower intensity. The high deformation cycles correspond to the interval during the deposition of the Sauce Grande Formation, decreasing in intensity towards the deposition period of the Bonete Formation

(nearly 300–290 Ma; Arzadún *et al.*, 2021). The second peak of deformation occurred during the early stage of deposition of the Tunas Formation (290–276 Ma), with lower intensity than the previous interval (Arzadún *et al.*, 2021). This spasmodic deformation is also reflected in the sharp cusp of the apparent polar wander path of Gondwana during the Early Paleozoic (Tomezzoli, 2009; Gallo *et al.*, 2017, Fig. 9). Further, the Permian deformation was again attenuated towards the foreland until the end of the Permian, during the last stage of deposition of the Tunas Formation (Tomezzoli, 1999, 2001, 2012; Arzadún *et al.*, 2016b, 2021; Febbo *et al.*, 2021).

7. Conclusions

The Tunas Formation represents the last depositional stage of the Claromecó Foreland Basin and constitutes a key piece to understand the evolution of the southwestern Gondwana margin, since it records

the paleogeographic and paleotectonic changes occurred during the Permian. Petrography and tectonic provenance studies were performed for the Tunas Formation sandstones, on subsurface (PANG 0001 and PANG 0003 wells) and outcrop samples (Gonzales Chavez locality) to determinate the paleotectonic scenario during its deposition.

Sandstones were classified as feldspathic litharenites and litharenites, with an average modal composition of Q49 F13 L38. Sandstone components are characterized by moderate to high content of quartz, high percentage of lithic fragments (predominantly metamorphic and volcanic rock fragments) and subordinate feldspars. Modal composition of sandstones from the Claromecó Basin area is distributed into the recycled orogen and transitional recycled to mixed fields. The provenance analysis result of this work is slightly different from those obtained by other authors (e.g., Andreis and Cladera 1992; López-Gamundí *et al.*, 1995; Alessandretti *et al.*, 2013; Ballivián Justiniano *et al.*, 2020) for outcrops in the Sierras Australes fold and thrust belt, which fall into the mixed to dissected arc fields. Differences could be attributed to different transport distances from the provenance area (Sierras Australes itself: Curamalal and Ventana groups) to the center of the basin, where feldspars could have been eroded by mechanical transportation.

Petrographic analyses, in addition to previous provenance and sedimentological studies, determine that sedimentary material was derived from a mixed source, which largely comes from the recycled orogen, with contributions of a volcanic source. This suggests that the Sierras Australes (located to the W–SW of the Claromecó Basin) was already uplifted as a fold and thrust belt, subjected to erosion and capable of supplying sedimentary material, particularly supplying metamorphic constituents, to the Claromecó Basin as a recycled orogeny. Sedimentation in the basin was coeval with volcanic activity, recorded by the intercalation of pyroclastic materials (tuff levels; Arzadún *et al.*, 2018) and sandstones with significant amounts of volcanic lithic grains interbedded in the siliciclastic sequence.

The synorogenic deposits of the Tunas Formation recorded a typical sedimentation of a foreland basin, developed along an active margin, characterized by the paleocurrent reversal and the dominance of fold belt/arc-derived material. The Tunas Formation shows clear differences in its modal composition, paleocurrent direction and paleoenvironmental condition with respect to the underlying units of the Pillahuincó Group. Source areas changed from

cratonic (Sauce Grande, Piedra Azul and Bonete formations) to mixed (Tunas Formation) fields, indicating the variations of the Claromecó Basin configuration during the Late Paleozoic. Changes on the paleotectonic scenario during the sedimentation period of Tunas Formation have been interpreted as the consequence of compressive post-collisional deformation, and, the product of adjustment, accommodation and translation of terranes and plates towards the equator during the Permian–Triassic, which forms the Pangea.

Funding

This work was co-funded by the “CIC–PIT–AP–BA 2016/17/18” and “SECYT–UNS (24/H144)” projects.

Availability of data and materials

The data that support the findings of this study are available on request from the corresponding author.

Authors' contributions

All the authors have actively participated in the preparation of the manuscript.

All authors read and approved the final proof.

Conflict of interest

The authors declare that they have no known competing financial interests or personal relationships that could have appeared to influence the work reported in this paper.

Acknowledgements

The authors thank the Departamento de Geología, Universidad Nacional del Sur, Bahía Blanca, for providing the equipment to carry out sample analyses. Special thanks to Dr. José Kostadinoff for his valuable contributions during fieldworks. We are grateful to the reviewers, Dr. Juan Pablo Lovecchio and Dr. Carlos Zavala, for their valuable suggestions and careful corrections of the manuscript, which have improved it considerably.

References

- Alessandretti, L., Philipp, R.P., Chemale, F., Brückmann, M.P., Zvirtes, G., Metté, V., Ramos, V.A., 2013. Provenance, volcanic record, and tectonic setting of the Paleozoic Ventania fold belt and the Claromecó foreland Basin: Implications on sedimentation and volcanism along the southwestern Gondwana margin. *Journal of South American Earth Sciences*, 47, 12–31. <https://doi.org/10.1016/j.jsames.2013.05.006>.
- Álvarez, G.T., 2004. *Cuencas Paleozoicas asociadas a la prolongación norte del sistema de Sierras de Ventania, Provincia de Buenos Aires*. PhD Thesis. Universidad Nacional del Sur, Argentina, p. 184.
- Álvarez, G.T., 2007. Extensión noroccidental de la Cuenca paleozoica de Claromecó, provincia de Buenos Aires. *Revista de la Asociación Geológica Argentina*, 62(1), 86–91.
- Andreis, R., Japas, M.S., 1991. Cuenca de Sauce Grande–Colorado. In: Archangelsky, S. (Ed.), *El Sistema Pérmico en la República Argentina y en la República Oriental del Uruguay*. Academia Nacional de Ciencias de Córdoba, Córdoba, pp. 45–65.
- Andreis, R.R., Archangelsky, S., González, C.R., López Gamundi, O., Sabattini, N., Aceñolaza, G., Azcuy, C.L., Cortiñas, J., Cuerda, A., Cúneo, R., 1987. Cuenca tepuel–genoa. In: Archangelsky, S. (Ed.), *El Sistema Carbonífero de la República Argentina*. Academia Nacional de Ciencias, Publicación Especial, pp. 169–196.
- Andreis, R.R., Cladera, G., 1992. Las epiclastitas pérmicas de la Cuenca Sauce Grande (Sierras Australes, Buenos Aires, Argentina). Parte 1: Composición y procedencia de los detritos. In: *IV Reunión de Sedimentología La Plata*, pp. 127–134.
- Andreis, R.R., Iñiguez Rodríguez, A.M., Lluch, J.J., Rodríguez, S., 1989. Cuenca paleozoica de Ventania. Sierras Australes de la provincia de Buenos Aires. In: Chebli, G., Spalletti, L. (Eds.), *Cuenca Sedimentarias Argentinas*. Serie Correlación Geológica, pp. 265–298.
- Andreis, R.R., Japas, M.S., 1996. Cuenca de Sauce Grande y Colorado. In: *12th International Congress on Carboniferous and Permian Stratigraphy and Geology and Academia Nacional de Ciencias, Córdoba*, pp. 45–64.
- Andreis, R.R., Lluch, J.J., Iñiguez Rodríguez, A.M., 1979. *Paleocorrientes y paleoambientes de las Formaciones Bonete y Tunas, Sierras Australes de la Provincia de Buenos Aires, Argentina*. VI Congreso Geológico Argentino, Buenos Aires, pp. 207–224.
- Archangelsky, S., Cúneo, R., 1984. Zonación del Pérmico continental de Argentina sobre la base de sus plantas fósiles. In: *III Congreso latinoamericano Paleontológico, Ciudad de México*, pp. 143–153.
- Arzadún, G., Cisternas, M.E., Cesaretti, N.N., Tomezzoli, R.N., 2016a. Análisis de la materia orgánica en niveles de carbón identificados en el pozo PANG0001, en la Formación Tunas (Pérmico de Gondwana), Cuenca de Claromecó, provincia de Buenos Aires. *Revista de la Asociación Geológica Argentina*, 73(4), 538–551.
- Arzadún, G., Cisternas, M.E., Cesaretti, N.N., Tomezzoli, R.N., 2017. Presence of charcoal as evidence of paleofires in the Claromecó Basin, Permian of Gondwana, Argentina: Diagenetic and paleoenvironment analysis based on coal petrography studies. *GeoResJ*, 14, 121–134. <https://doi.org/10.1016/j.grj.2017.11.001>.
- Arzadún, G., Lovecchio, J.P., Becchio, R., Uriz, N.J., Cingolani, C., Febbo, M.B., Hernandez, R., Bolatti, N., Kress, P., 2020. Thermochronology of the Ventana ranges and Claromecó Basin, Argentina: Record of Gondwana breakup and South Atlantic passive margin dynamics. *Journal of South American Earth Sciences*, 105, 102965. <https://doi.org/10.1016/j.jsames.2020.102965>.
- Arzadún, G., Tomezzoli, R.N., Cesaretti, N.N., 2016b. Tectonic insight based on anisotropy of magnetic susceptibility and compaction studies in the Sierras Australes thrust and fold belt (southwest Gondwana boundary, Argentina). *Tectonics*, 35, 1015–1031. <https://doi.org/10.1002/2015TC003976>.
- Arzadún, G., Tomezzoli, R.N., Fortunatti, N., Cesaretti, N.N., Febbo, M.B., Calvagno, J.M., 2021. Deformation understanding in the Upper Paleozoic of Ventana ranges at southwest Gondwana boundary. *Scientific Reports*, 11, 20804. <https://doi.org/10.1038/s41598-021-99087-1>.
- Arzadún, G., Tomezzoli, R.N., Trindade, R., Gallo, L.C., Cesaretti, N.N., Calvagno, J.M., 2018. Shrimp zircon geochronology constrains on Permian pyroclastic levels, Claromecó Basin, south-west margin of Gondwana, Argentina. *Journal of South American Earth Sciences*, 85, 191–208.
- Azcuy, C.L., Caminos, R., 1987. Diametrofismo. In: Archangelsky, S. (Ed.), *El Sistema Carbonífero en la República Argentina*. Academia Nacional de Ciencias, pp. 239–251.
- Ballivián Justiniano, C.A., Comerio, M.A., Gerónimo, O., Sato, A.M., Coturel, E.P., Naipauer, M., Basei, M.A.S., 2020. Geochemical, palaeontological, and sedimentological approaches of a syn-orogenic clastic wedge: Implications for the provenance of the Permian (Cisuralian) Tunas Formation, Ventania System (Argentina). *Journal of South American Earth Sciences*, 104, 102836. <https://doi.org/10.1016/j.jsames.2020.102836>.
- Bangert, B., Stolhofen, H., Lorenz, V., Armstrong, R.I., 1999. The geochronology and significance of ash fall tuffs in the glacigenic, Carboniferous–Permian Dwyka Group of Namibia and South Africa. *Journal of African Earth Sciences*, 29, 33–49.
- Buggisch, W., 1987. Stratigraphy and very low grade metamorphism of the Sierras Australes of the province of Buenos Aires, Argentina and implications in Gondwana correlations. *Zentralblatt Mineralogie Geologie Paläontologie*, 1, 819–837.
- Catuneanu, O., Hancox, P.J., Rubidge, B.S., 1998. Reciprocal flexural behaviour and contrasting stratigraphies: A new basin development model for the Karoo retroarc foreland system, South Africa. *Basin Research*, 10, 417–439.
- Cobbold, P.R., Gapais, D.A., Rossello, E.A., 1991. Partitioning of transpressive motions within a sigmoidal foldbelt: The Variscan Sierras Australes, Argentina. *Journal of Structural Geology*, 13, 743–758.

- Cobbold, P.R., Massabie, A., Rossello, E.A., 1986. Hercynian wrenching and thrusting in the Sierras Australes foldbelt, Argentina. *Hercynica*, II, 2, 135–148.
- Critelli, S., Ingersoll, R.V., 1995. Interpretation of neovolcanic versus palaeovolcanic sand grains: An example from Miocene deep-marine sandstone of the Topanga Group (Southern California). *Sedimentology*, 42, 783–804.
- Datta, B., 2005. Provenance, tectonics and palaeoclimate of Proterozoic Chandarpur sandstones, Chattisgarh Basin: A petrographic view. *Journal of Earth System Science*, 114, 227–245.
- De Ros, L., Morad, S., Al-Aasm, I., 1997. Diagenesis of siliciclastic and volcaniclastic sediments in the Cretaceous and Miocene sequences of the NW African margin (DSDP Leg 47A, site 397). *Sedimentary Geology*, 112, 137–156.
- De Wit, M.J., Jeffery, M., Bergh, H., Nicolaysen, L., 1988. *Geological Map of Sectors of Gondwana, Reconstructed to Their Disposition — 150 Ma*. American Association of Petroleum Geologists, Tulsa, USA.
- DeCelles, P.G., 1986. Sedimentation in a tectonically partitioned, nonmarine foreland basin: The Lower Cretaceous Kootenai Formation, southwestern Montana. *The Geological Society of America Bulletin*, 97, 911–921.
- DeCelles, P.G., Hertel, F., 1989. Petrology of fluvial sands from the Amazonian foreland basin, Peru and Bolivia. *The Geological Society of America Bulletin*, 101, 1552–1562.
- di Pasquo, M., Di Nardo, J., Martínez, M., Arzadún, G., Silvestri, L., 2018. Análisis palinoestratigráfico de muestras de subsuelo de la Formación Tunas (Pérmino), Cuenca de Claromecó, Provincia de Buenos Aires, Argentina. In: *XVII Simposio Argentino de Palinología y Paleobotánica, Boletín de la Asociación Latinoamericana de Paleobotánica y Palinología, Paraná*, pp. 77–78.
- di Pasquo, M., Martínez, M.A., Freije, H., 2008. Primer registro palinológico de la Formación Sauce Grande (Pennsylvaniano–Cisuraliano) en las Sierras Australes, provincia de Buenos Aires, Argentina. *Ameghiniana*, 45(1), 69–81.
- Dickinson, W., Beard, L., Brakenridge, G., Erjavec, J., Ferguson, R., Inman, K., Kneppe, R., Lindberg, F., Ryberg, P., 1983. Provenance of North American Phanerozoic sandstones in relation to tectonic setting. *The Geological Society of America Bulletin*, 94, 222–235.
- Dickinson, W.R., 1970. Interpreting detrital modes of graywacke and arkose. *Journal of Sedimentary Petrology*, 40, 695–707.
- Dickinson, W.R., Suczek, C.A., 1979. Plate tectonics and sandstone compositions. *American Association of Petroleum Geologists Bulletin*, 63(12), 2164–2182.
- Du Toit, A.L., 1927. *A Geological Comparison of South America with South Africa*, vol. 381. Carnegie Institution of Washington Publication, pp. 1–157.
- Febbo, M.B., Arzadún, G., Cesaretti, N.N., Tomezzoli, R.N., Fortunatti, N., 2022. The Claromecó Frontier Basin: Hydrocarbon source rock potential of the Tunas Formation, southwestern Gondwana margin, Argentina. *Marine and Petroleum Geology*, 137, 105491. <https://doi.org/10.1016/j.marpetgeo.2021.105491>.
- Febbo, M.B., Choque, G., Cesaretti, N.N., Tomezzoli, R.N., Kostadinoff, J., 2018b. Análisis de facies y petrografía de la Formación Tunas en el área de Gonzales Chaves, Cuenca de Claromecó, provincia de Buenos Aires, Argentina. In: *XVI Reunión Argentina de Sedimentología, Abstracts. General Roca*, p. 48.
- Febbo, M.B., Fortunatti, N., Cesaretti, N.N., Arzadún, G., Tomezzoli, R.N., 2018a. Evolución diagenética de la Formación Tunas para el pozo PANG 0001, Cuenca de Claromecó, provincia de Buenos Aires, Argentina: Su potencial como reservorio de hidrocarburos. In: *Actas X Congreso de Exploración y Desarrollo de Hidrocarburos, Mendoza*, pp. 763–779.
- Febbo, M.B., Fortunatti, N.B., Arzadún, G., Cesaretti, N.N., Tomezzoli, R.N., 2017. Análisis de facies de subsuelo y su potencial oleogenético para el pozo PANG 0001, Formación Tunas, Pérmico de la Cuenca de Claromecó, Provincia de Buenos Aires. In: *Actas XX Congreso Geológico Argentino. San Miguel de Tucumán*, pp. 27–33.
- Febbo, M.B., Tomezzoli, R.N., Calvagno, J.M., Arzadún, G., Gallo, L., Cesaretti, N.N., 2021. Anisotropy of magnetic susceptibility analysis in Tunas Formation cores (Permian), Claromecó Basin, Buenos Aires, Argentina: Its relation to depositional and post-depositional conditions. *Journal of South American Earth Sciences*, 107, 103144. <https://doi.org/10.1016/j.jsames.2020.103144>.
- Folk, R.L., Andrews, P.B., Lewis, D.W., 1970. Detrital sedimentary rock classification and nomenclature for use in New Zealand. *New Zealand Journal of Geology and Geophysics*, 13, 937–968.
- Fryklund, B., Marshall, A., Stevens, J., 1996. Cuenca del Colorado. In: Ramos, V.A., Turic, M.A. (Eds.), *XIII Congreso Geológico Argentino and III Congreso de Exploración de Hidrocarburos (Buenos Aires, Argentina)*. Geología y Recursos Naturales de la Plataforma Continental Argentina, Relatorio, pp. 135–158.
- Furque, G., 1965. *Nuevos afloramientos del Paleozoico en la provincia de Buenos Aires*, vol. 5. Revista Museo de La Plata, pp. 239–243.
- Gallo, L.C., Farjat, A.D., Tomezzoli, R.N., Calvagno, J.M., Hernández, R.M., 2020. Sedimentary evolution of a Permo-Carboniferous succession in southern Bolivia: Responses to icehouse-greenhouse transition from a probabilistic assessment of paleolatitude. *Journal of South American Earth Sciences*, 106, 102923. <https://doi.org/10.1016/j.jsames.2020.102923>.
- Gallo, L.C., Tomezzoli, R.N., Cristallini, E.O.A., 2017. Pure dipole analysis of the Gondwana apparent polar wander path: Paleogeographic implications in the evolution of Pangea. *Geochemistry, Geophysics, Geosystems*, 18, 1499–1519.
- Gregori, D.A., Kostadinoff, J., Strazzere, L., Raniolo, A., 2008. Tectonic significance and consequences of the Gondwanide orogeny in northern Patagonia, Argentina. *Gondwana Research*, 14, 429–450. <https://doi.org/10.1016/j.gr.2008.04.005>.
- Guerra-Sommer, M., Cazzullo-Klepzig, M., Formoso, M.L.L., Menegat, R., Basei, M.A.S., 2005. New radiometric data from ash fall rocks in Candiota coal-bearing strata and the palynostratigraphic framework in southern Paraná Basin (Brazil). In: Pankhurst, R.J., Veiga, G.D. (Eds.), *Gondwana Mendoza*, p. 89.
- Harrington, H.J., 1947. *Explicación de las Hojas Geológicas 33m y 34m, Sierras de Curamalal y de la Ventana*,

- Provincia de Buenos Aires*, vol. 61. Servicio Nacional de Minería y Geología, Buenos Aires, p. 43.
- Harrington, H.J., 1970. Las Sierras Australes de Buenos Aires, república Argentina: Cadena autocogénica. *Revista de la Asociación Geológica Argentina*, 25(2), 151–181.
- Harrington, H.J., 1972. Sierras Australes de Buenos Aires. In: Leanza, A.F. (Ed.), *Geología Regional Argentina*. Academia Nacional de Ciencias, Córdoba, Argentina, pp. 395–405.
- Ingersoll, R.V., Bulard, T.F., Ford, R.L., Grimm, J.P., Pickle, J.P., Sares, S.W., 1984. The effect of grain size on detrital modes: A test of the gazzi-dickinson point counting method. *Journal of Sedimentary Petrology*, 54, 103–116.
- Introcaso, A., 1982. *Características de la corteza en el positivo bonaerense: Tandilia-Cuenca Interserrana-Ventania a través de datos de gravedad*. Observatorio Astronómico Municipalidad de Rosario, Publicación del Instituto de Física de Rosario, Rosario, pp. 1–6.
- Iñíguez, A.M., Andreis, R.R., Zalba, A.A., 1988. Eventos piroclásticos en la Formación Tunas (Pérmino), Sierras Australes, provincia de Buenos Aires, República Argentina. In: *II Jornadas Geológicas Bonaerenses*. Bahía Blanca, pp. 383–395.
- Japas, M.S., 1989. *La deformación de la cadena plegada de las Sierras Australes de la provincia de Buenos Aires*. Academia Nacional de Ciencias Exactas Físicas y Naturales, Buenos Aires, pp. 193–215.
- Keidel, J., 1916. La geología de las Sierras de la provincia de Buenos Aires y sus relaciones con las montañas del Cabo y los Andes. In: *Ministerio de agricultura de la Nación. Sección Geología, Mineralogía y Minería*. Anales, Buenos Aires, pp. 5–57, 9 (3).
- Keidel, J., 1921. Sobre la distribución de los depósitos glaciares del Pérmino conocidos en la Argentina y su significación para la estratigrafía de la serie del Gondwana y la paleogeografía del Hemisferio Austral. *Academia Nacional de Ciencias*, 25, 239–368.
- Kostadinoff, J., 1993. Geophysical evidence of a Paleozoic basin in the interhilly area of Buenos Aires province, Argentina. *Comptes Rendus XII ICCP*, 1, 397–404.
- Kostadinoff, J., 2007. Evidencia geofísica del umbral de Trenque Lauquen en la extensión norte de la Cuenca de Claromecó, Provincia de Buenos Aires. *Revista de la Asociación Geológica Argentina*, 62(1), 69–75.
- Kostadinoff, J., Font de Affolter, G., 1982. *Cuenca Interserrana Bonaerense, Argentina*, vol. 4. V Congreso Latinoamericano de Geología, Buenos Aires, pp. 105–121.
- Lesta, P., Sylwan, C., 2005. Cuenca de Claromecó. In: *VI Congreso de Exploración y Desarrollo de Hidrocarburos, Simposio Frontera Exploratoria de la Argentina, Mar del Plata*, pp. 217–231.
- Lesta, P.J., Turic, M.A., Mainardi, E., 1978. Actualización de la información estratigráfica en la Cuenca de Colorado. In: *VII Congreso Geológico Argentino. Neuquén*, pp. 701–713.
- Limarino, C.O., Césari, S.N., Spalletti, L.A., Taboada, A.C., Isbell, J.L., Geuna, S., Gulbranson, E.L., 2014. A paleoclimatic review of southern South America during the Late Paleozoic: A record from icehouse to extreme greenhouse conditions. *Gondwana Research*, 25, 1396–1421. <https://doi.org/10.1016/j.gr.2012.12.022>.
- Llambías, E.J., Prozzi, C.R., 1975. Ventania. In: *VI Congreso Geológico Argentino. Relatorio*, Buenos Aires, pp. 79–102.
- López-Gamundí, O.R., 2006. Permian plate margin volcanism and tuffs in adjacent basins of west Gondwana: Age constraints and common characteristics. *Journal of South American Earth Sciences*, 22, 227–238. <https://doi.org/10.1016/j.jsames.2006.09.012>.
- López-Gamundí, O.R., Conaghan, P.J., Rossello, E.A., Cobbold, P.R., 1995. The Tunas Formation (Permian) in the Sierras Australes foldbelt, east central Argentina: Evidence for syntectonic sedimentation in a foreland Basin. *Journal of South American Earth Sciences*, 8(2), 129–142. [https://doi.org/10.1016/0895-9811\(95\)00001-V](https://doi.org/10.1016/0895-9811(95)00001-V).
- López-Gamundí, O.R., Espejo, I.S., Conaghan, P.J., Powell, C.McA., 1994. Southern South America. *The Geological Society of America Bulletin*, 184, 281–330.
- López-Gamundí, O.R., Fildani, A., Weislogel, A., Rossello, E., 2013. The age of the Tunas Formation in the Sauce Grande basin–Ventana foldbelt (Argentina): Implications for the Permian evolution of the southwestern margin of Gondwana. *Journal of South American Earth Sciences*, 45, 250–258.
- López-Gamundí, O.R., Rossello, E.A., 1992. La Cuenca interserrana (Claromecó) de Buenos Aires, Argentina: Un ejemplo de cuenca hercínica de antepaís. In: *III Congreso Geológico de España and VIII Congreso Latinoamericano de Geología*, Salamanca, pp. 55–59.
- López-Gamundí, O.R., Rossello, E.A., 1998. Basin fill evolution and paleotectonic patterns along the Samfrau geosyncline: The Sauce Grande BasineVentana foldbelt (Argentina) and Karoo Basin–Cape Foldbelt (South Africa) revisited. *Geologische Rundschau*, 86, 819–834.
- López-Gamundí, O.R., Rossello, E.A., 2021. The Permian Tunas Formation (Claromecó Basin, Argentina): Potential naturally fractured reservoir and/or coal bed methane (CBM) play? *Marine and Petroleum Geology*, 128, 1–14. <https://doi.org/10.1016/j.marpetgeo.2021.104998>.
- Lovecchio, J.P., Rohais, S., Joseph, P., Bolatti, N.D., Kress, P.R., Gerster, R., Ramos, V.A., 2018. Multistage rifting evolution of the Colorado basin (offshore Argentina): Evidence for extensional settings prior to the South Atlantic opening. *Terra Nova*, 30, 359–368. <https://doi.org/10.1111/ter.12351>.
- Lovecchio, J.P., Rohais, S., Joseph, P., Bolatti, N.D., Ramos, V.A., 2020. Mesozoic rifting evolution of SW Gondwana: A poly-phased, subduction-related, extensional history responsible for basin formation along the Argentinean Atlantic margin. *Earth- Sciences Reviews*, 203, 103–138.
- McBride, E.F., 1985. Diagenetic processes that affect provenance determinations in sandstones. In: Zuffa, G.G. (Ed.), *Provenance of Arenites*, vol. 148. NATO ASI Series, Reidel, Dordrecht, pp. 95–113.
- Milani, E.J., De Wit, M.J., 2008. *Correlations between the Classic Paraná and Cape Karoo Sequences of South America and Southern Africa and Their Basin Flanking*

- the Gondwanides: Du Toit Revisited*, vol. 294. Geological Society, London, Special Publications, pp. 319–342.
- Monteverde, A., 1937. Nuevo yacimiento de material pétreo en González Chaves. *Revista Minera*, 8, 116–124.
- Morad, S., Al-Ramadan, K., Ketzer, M., De Ros, L., 2010. The impact of diagenesis on the heterogeneity of sandstone reservoirs: A review of the role of depositional facies and sequence stratigraphy. *AAPG Bulletin*, 94(8), 1267–1309.
- Pángaro, F., Ramos, V.A., Pazos, P.J., 2015. The Hesperides basin: A continental-scale Upper Paleozoic to Triassic basin in southern Gondwana. *Basin Research*, 28, 685–711. <https://doi.org/10.1111/bre.12126>.
- Pángaro, F., Ramos, V.A., 2012. Paleozoic crustal blocks of onshore and offshore central Argentina: New pieces of the southwestern Gondwana collage and their role in the accretion of Patagonia and the evolution of Mesozoic South Atlantic sedimentary basins. *Marine and Petroleum Geology*, 37(1), 162–183. <https://doi.org/10.1016/j.marpetgeo.2012.05.010>.
- Ramos, V.A., 1984. Patagonia: Un nuevo continente paleozoico a la deriva?. In: *IX Congreso Geológico Argentino, Bariloche*, pp. 311–325.
- Ramos, V.A., 2008. Patagonia: A Paleozoic continental drift? *Journal of South American Earth Sciences*, 26, 235–251. <https://doi.org/10.1016/j.jsames.2008.06.002>.
- Ramos, V.A., Kostadinoff, J., 2005. La cuenca de Claromecó. In: de Barrio, R.E., Echeverri, R.O., Caballé, M.F., Llambías, E. (Eds.), *Geología y recursos minerales de la provincia de Buenos Aires. XVI Congreso Geológico Argentino, Relatorio, La Plata*, pp. 473–480.
- Ramos, V.A., Naipauer, M., 2014. Patagonia: Where does it come from? *Journal of Iberian Geology*, 40, 367–379. https://doi.org/10.5209/rev_JIGE.2014.v40.n2.45304.
- Ramos, V.A., Chemale, F., Naipauer, M., Pazos, P.J., 2014. A provenance study of the Paleozoic Ventania System (Argentina): Transient complex sources from western and eastern Gondwana. *Gondwana Research*, 26, 719–740. <https://doi.org/10.1016/j.gr.2013.07.008>.
- Rocha-Campos, A.C., Basei, A.C., Nutman, M.A.S., Santos, P.R., 2006. SHRIMP U–Pb zircon geochronological calibration of the Late Paleozoic supersequence, Paraná Basin, Brazil. In: *5th South American Symposium on Isotope Geology, Punta del Este, Uruguay*, p. 322.
- Rocha-Campos, A.C., Basei, M.A.S., Nutman, A.P., Kleiman, L.E., Varela, R., Llambías, E., Canile, F.M., da Rosa, O., 2011. 30 million years of Permian volcanism recorded in the Choiyoi igneous province (W Argentina) and their source for younger ash fall deposits in the Paraná Basin: SHRIMP U–Pb zircon geochronology evidence. *Gondwana Research*, 19, 509–523.
- Rocha-Campos, A.C., dos Santos, P.R., Canuto, J.R., 2008. Late Paleozoic glacial deposits of Brazil: Paraná basin. In: Fielding, C.R., Frank, T.D., Isbell, J.L. (Eds.), *Resolving the Late Paleozoic Ice Age in Time and Space*, vol. 441. Geological Society of America Special Paper, pp. 97–114.
- Sato, A.M., Llambías, E.J., Basei, M.A.S., Castro, C.E., 2015. Three stages in the Late Paleozoic to Triassic magmatism of southwestern Gondwana, and the relationships with the volcanic events in coeval basins. *Journal of South American Earth Sciences*, 63, 48–69. <https://doi.org/10.1016/j.jsames.2015.07.005>.
- Stolhofen, H., Stanistreet, L.G., Bangert, B., Grill, H., 2000. Tuffs, tectonism and glacially related sea-level changes, Carboniferous–Permian southern Namibia. *Palaeogeography, Palaeoclimatology, Palaeoecology*, 161, 127–150.
- Suero, T., 1972. Compilación geológica de las Sierras Australes de la provincia de Buenos Aires. *LEMIT (La Plata)*, 3, 135–147.
- Tohver, E., Weil, A.B., Solum, J.G., Hall, C.M., 2008. Direct dating of chemical remagnetizations in sedimentary rocks, insights from clay mineralogy and $^{40}\text{Ar}/^{39}\text{Ar}$ age analysis. *Earth and Planetary Science Letters*, 274, 524–530.
- Tomezzoli, R.N., 1999. La Formación Tunas en las Sierras Australes de la Provincia de Buenos Aires. Relaciones entre sedimentación y deformación a través de su estudio paleomagnético. *Revista de la Asociación Geológica Argentina*, 54(3), 220–228.
- Tomezzoli, R.N., 2001. Further palaeomagnetic results from the Sierras Australes fold and thrust belt, Argentina. *Geophysical Journal International*, 147, 356–366. <https://doi.org/10.1046/j.0956-540x.2001.01536.x>.
- Tomezzoli, R.N., 2009. The apparent polar wander path for South America during the Permian–Triassic. *Gondwana Research*, 15, 209–215. <https://doi.org/10.1016/j.gr.2008.10.005>.
- Tomezzoli, R.N., 2012. Chilenia y Patagonia: Un mismo continente a la deriva? *Revista de la Asociación Geológica Argentina*, 69(2), 222–239.
- Tomezzoli, R.N., Cristallini, E.O., 1998. Nuevas evidencias sobre la importancia del fallamiento en la estructura de las Sierras Australes de la provincia de Buenos Aires. *Revista de la Asociación Geológica Argentina*, 53, 117–129.
- Tomezzoli, R.N., Tickyj, H., Febbo, B., Calvagno, J.M., Gallo, L.C., Arzadún, A., Copertini, F., Ochoa, J., Battler, J.M., 2019. Following the steps of CHI–PA. In: *Latinmag Letters*, vol. 9. Proceedings Rancagua, Chile, pp. 1–6.
- Tomezzoli, R.N., Tickyj, H., Rapalini, A.E., Gallo, L.C., Cristallini, E.O., Arzadun, G., Chemale Jr, F., 2018. Gondwana's apparent polar wander path during the Permian — new insights from south America. *Scientific Reports*, 8, 8436. <https://doi.org/10.1038/s41598-018-25873-z>.
- Tomezzoli, R.N., Vilas, J.F., 1997. Paleomagnetismo y fábrica magnética en afloramientos cercanos a las Sierras Australes de la Provincia de Buenos Aires (López Lecube y González Chaves). *Revista de la Asociación Geológica Argentina*, 52(4), 419–432.
- Tomezzoli, R.N., Vilas, J.F., 1999. Paleomagnetic constraints on age of deformation of the Sierras Australes thrust and fold belt, Argentina. *Geophysical Journal International*, 138, 857–870.
- Vazquez Lucero, S.E., Prezzi, C., Scheck-Wenderoth, M., Bott, J., Gomez Dacal, M.L., Balestrini, F.I., Vizán, H., 2020. 3D gravity modelling of Colorado and Claromecó basins: New evidences for the evolution of the southwestern margin of Gondwana. *International Journal of Earth Sciences*, 110, 2295–2313. <https://doi.org/10.1007/s00531-020-01944-3>.

- Vizán, H., Prezzi, C., Japas, M.S., Van Zele, M.A., Geuna, S.E., Renda, E.M., 2015. Slab pull in the northern margin of Paleotethys ocean and internal deformation in Gondwana (including Ventana fold belt). *Revista de la Asociación Geológica Argentina*, 72(3), 355–377.
- von Gosen, W., Buggisch, W., Krumm, S., 1991. Metamorphism and deformation mechanisms in the Sierras Australes fold and thrust belt (Buenos Aires province, Argentina). *Tectonophysics*, 185, 335–356. [https://doi.org/10.1016/0040-1951\(91\)90453-Y](https://doi.org/10.1016/0040-1951(91)90453-Y).
- Zavala, C., Torresi, A., Zorzano, A., Arcuri, M., Di Meglio, M., 2019. Análisis sedimentológico y estratigráfico de la Formación Tunas (Pérmino, Cuenca de Claromecó). Estudio de subsuelo de los pozos PANG0001 y PANG0003. *Revista de la Asociación Geológica Argentina*, 76(3), 296–314.
- Zavala, C.A., Santiago, M.F., Amaolo, G.E., 1993. Depósitos fluviales en la Formación Tunas (Pérmino). Cuenca Paleozoica de Ventania, provincia de Buenos Aires. *Revista de la Asociación Geológica Argentina*, 48, 307–316.
- Zorzano, A., Di Meglio, M., Zavala, C., Arcuri, M.J., 2011. La Formación Tunas (Pérmino) en la Cuenca Interserrana. Primera correlación entre campo y subsuelo mediante registros de rayos gamma. In: XVIII Congreso Geológico Argentino, Neuquén, pp. 2–6.
- Zuffa, G.G., Cibin, U., Di Giulio, A., 1995. Arenite petrography in sequence stratigraphy. *The Journal of Geology*, 103, 451–459.